



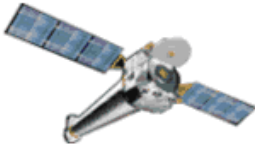
Chandra Flight Note

FLIGHT NOTE NO.	439
SUBJECT	2003:319 Attitude Disturbance
DATE	29 June 2004
AUTHOR	S. Bucher / E. Martin

Overview and Initial Checks

Routine checks of the Spacecraft Engineering Daily Plots showed a disturbance in the pointing stability just before 16:00 UT on 2003:319 (**Figure 1**). The daily limit exception file and remaining daily plots were checked for any other indications of unusual behavior. The other PCAD daily plots are: One-shot Attitude Update (**Figure 2**), Sun Sensors (**Figure 3**), Gyro Bias (**Figure 4**), Gyro Current (**Figure 5**), Gyro Temperatures, Maneuvers (**Figure 6**), Reaction Wheel Temperatures and Speeds (large scale), Reaction Wheel Torque Currents (**Figure 7**) and Stars (**Figure 8**). The one-shot plot showed an event not associated with the end of a maneuver at the same time as the pointing stability disturbance, but all of the remaining plots were nominal. The Propulsion System Momentum plot was also checked, and appeared nominal (see **Figures 13** and **14** for momentum plots).

Once the daily plots showed nominal behavior from the hardware, the cause of the pointing stability disturbance was investigated. Items such as an HRC door move while in Normal Pointing Mode (NPM) or a SIM translation associated with an SCS 107 run will produce disturbances in the pointing stability and an unexpected one-shot. Therefore, the first course of action was to check the daily loads for any mechanism commanding and to verify that SCS 107 had not run. There was no commanding in the daily loads within an hour of the disturbance and SCS 107 had not run. This prompted a more through investigation. The investigation ruled out all internal causes. The disturbance occurred during the yearly Leonid meteoroid shower. Since analysis ruled out a cause internal to the spacecraft for the disturbance, it was hypothesized that the spacecraft was struck by a Leonid or other micrometeoroid. The other subsystem engineers were contacted and asked to do a detailed check of the health and status of their subsystems. These checks showed no anomalous behavior.



Chandra Flight Note

14:52:19 Z

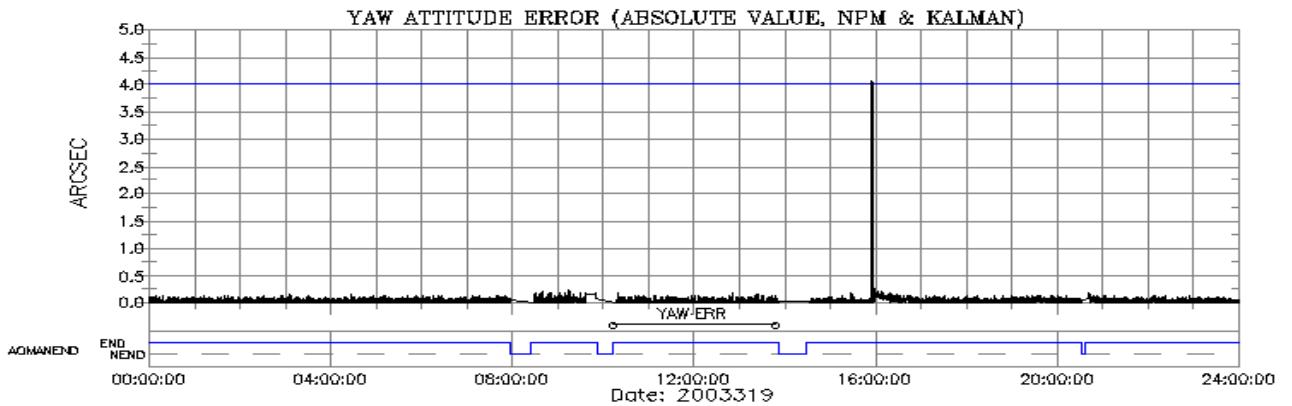
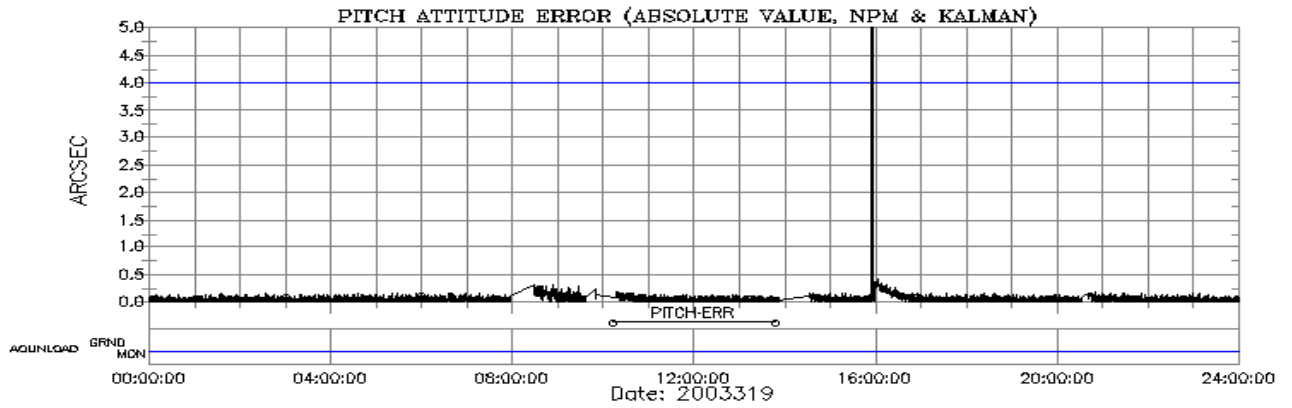


Figure 1: Pointing Stability

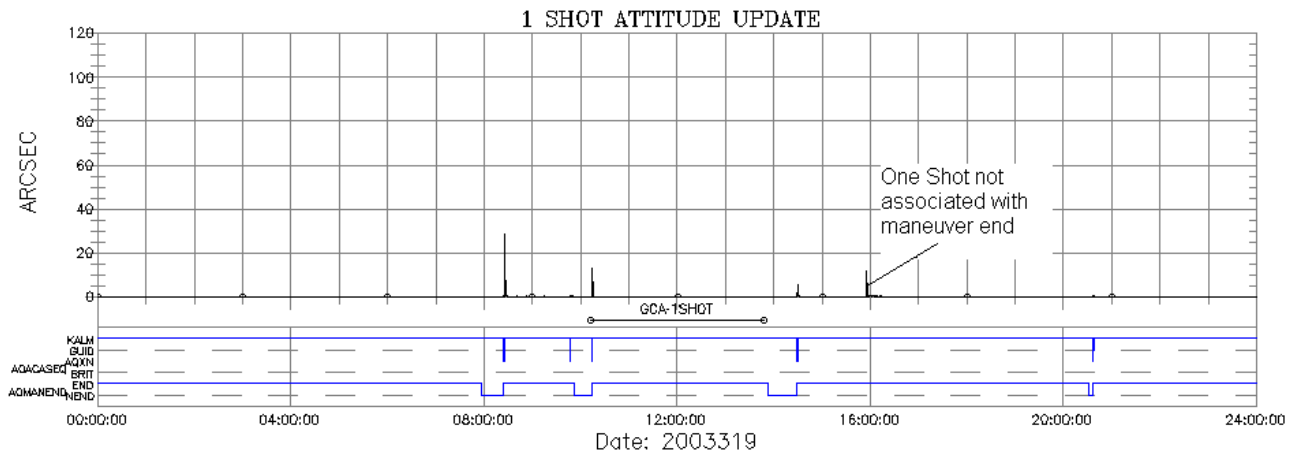


Figure 2: One-shot Attitude Update

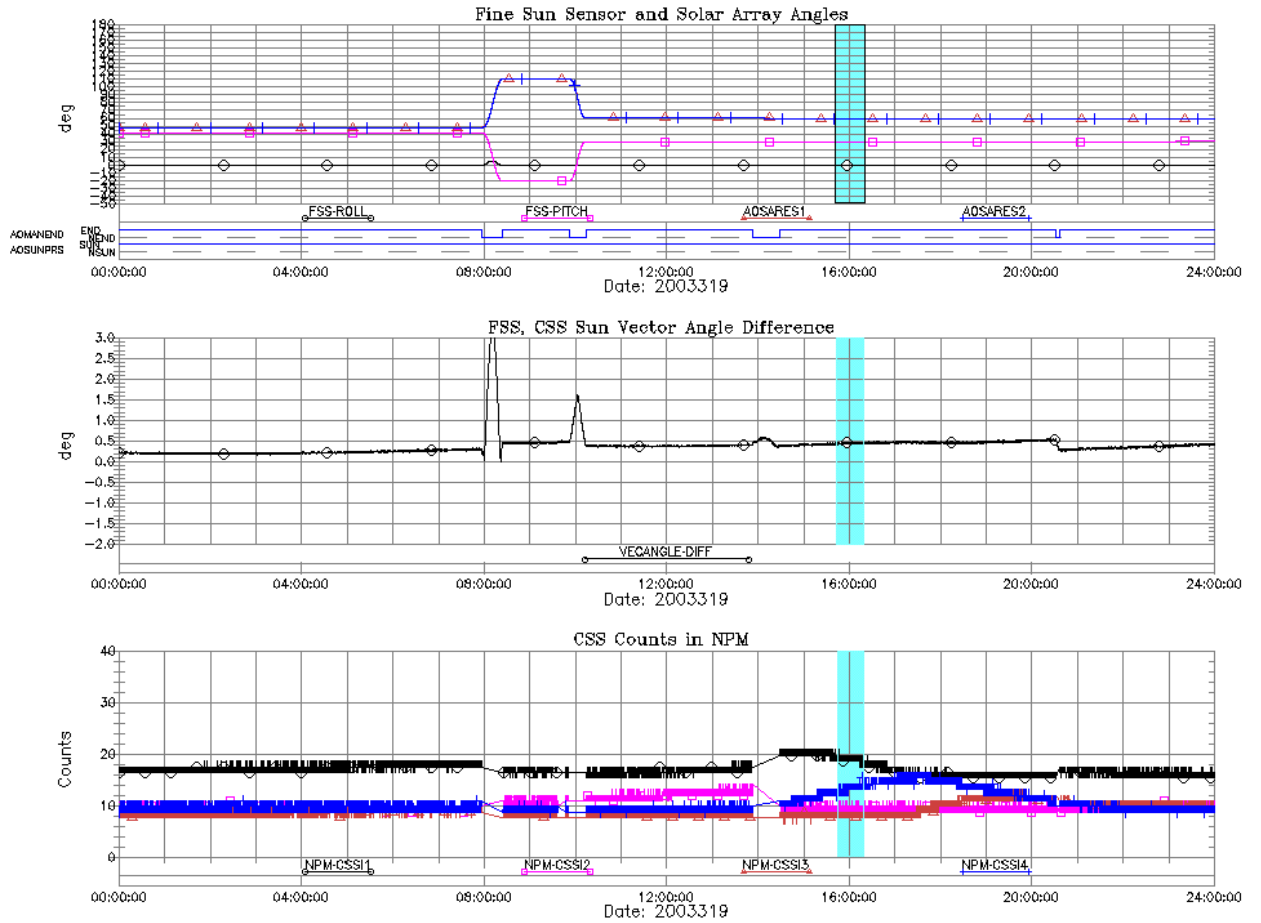


Figure 3: Sun Sensors

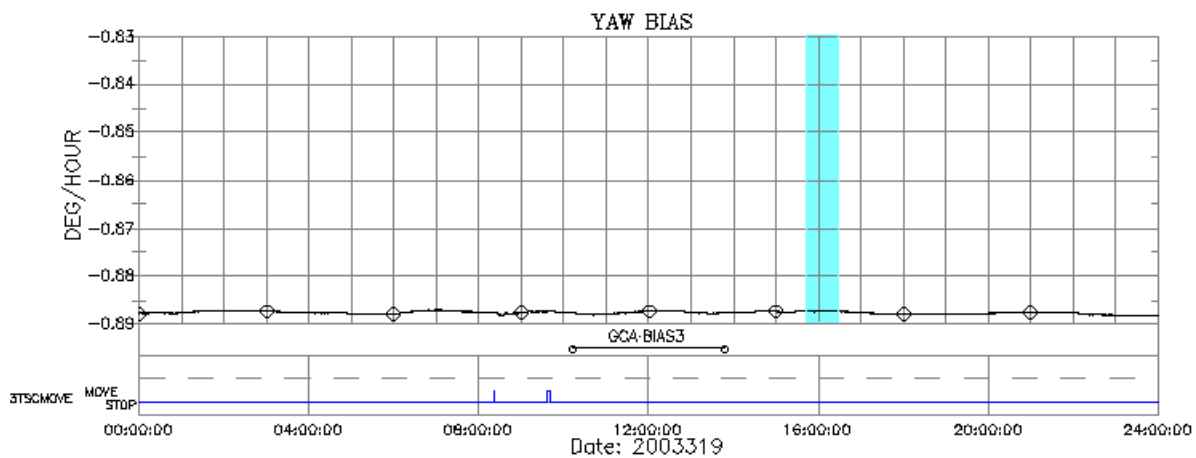
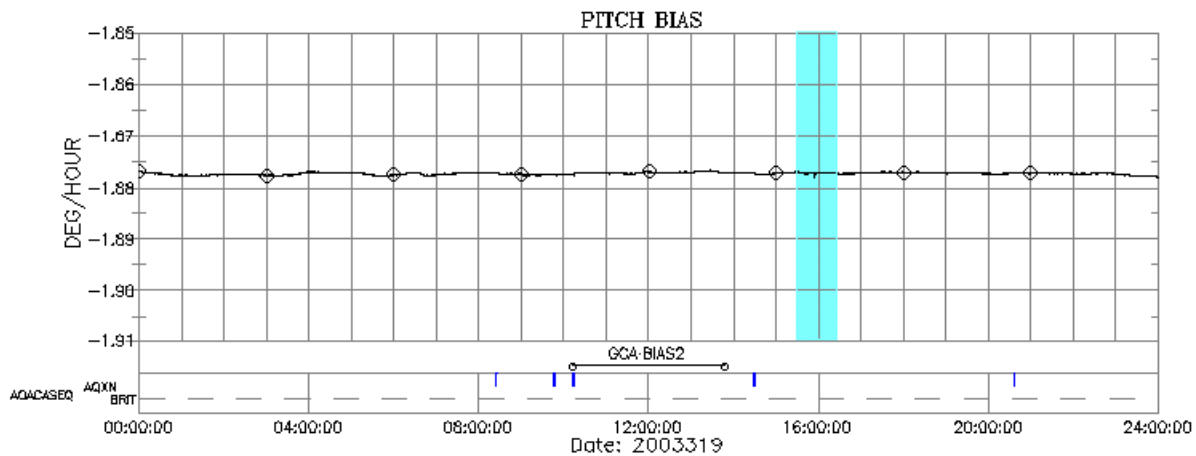
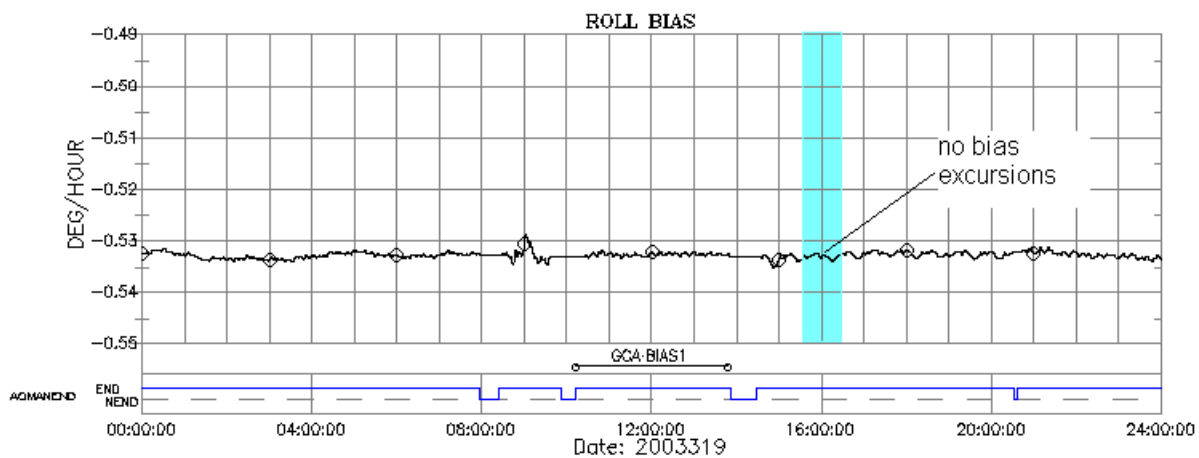


Figure 4: Gyro Bias

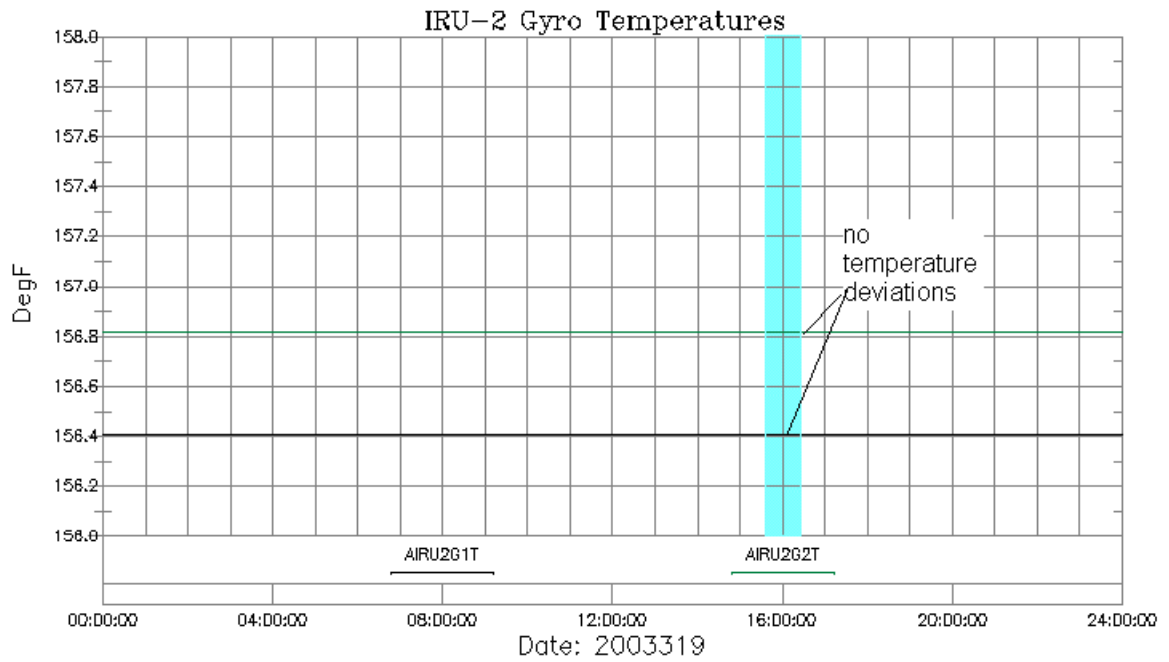
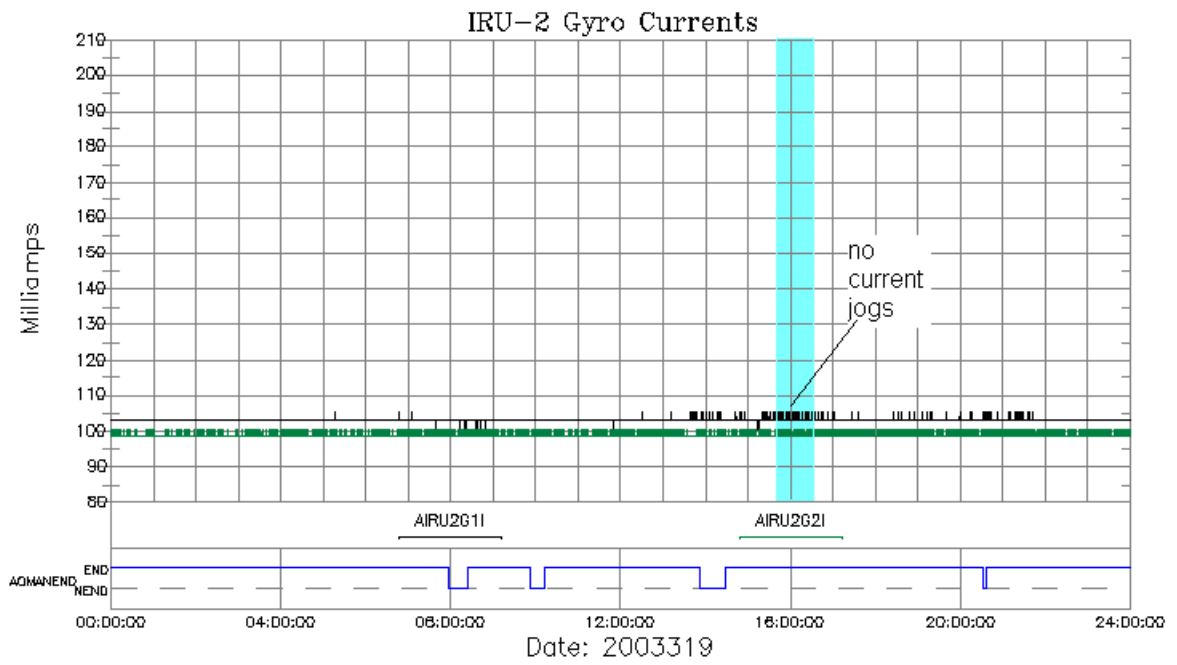


Figure 5: Gyro Health (Current and Temperature)

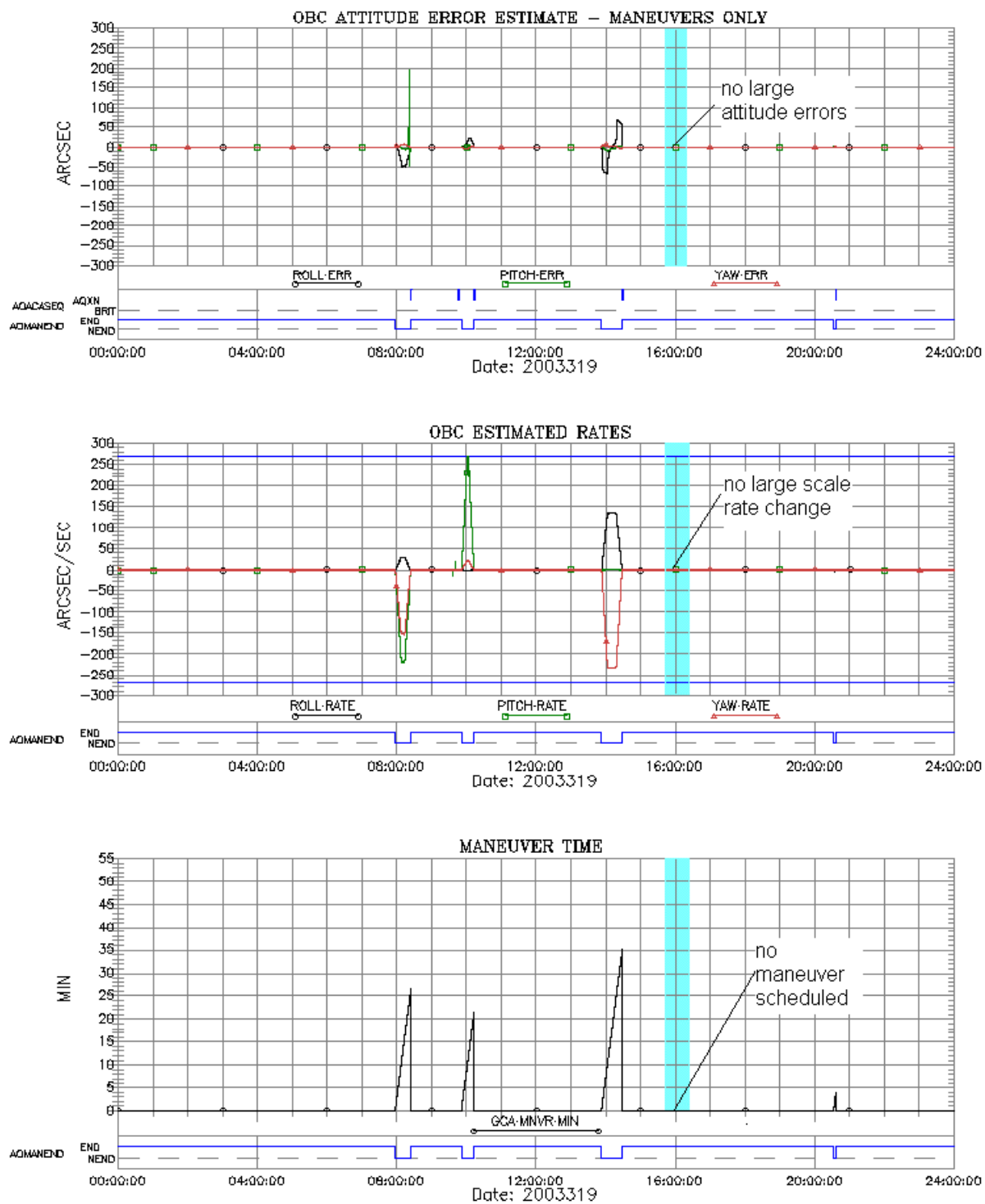


Figure 6: Maneuver Parameters

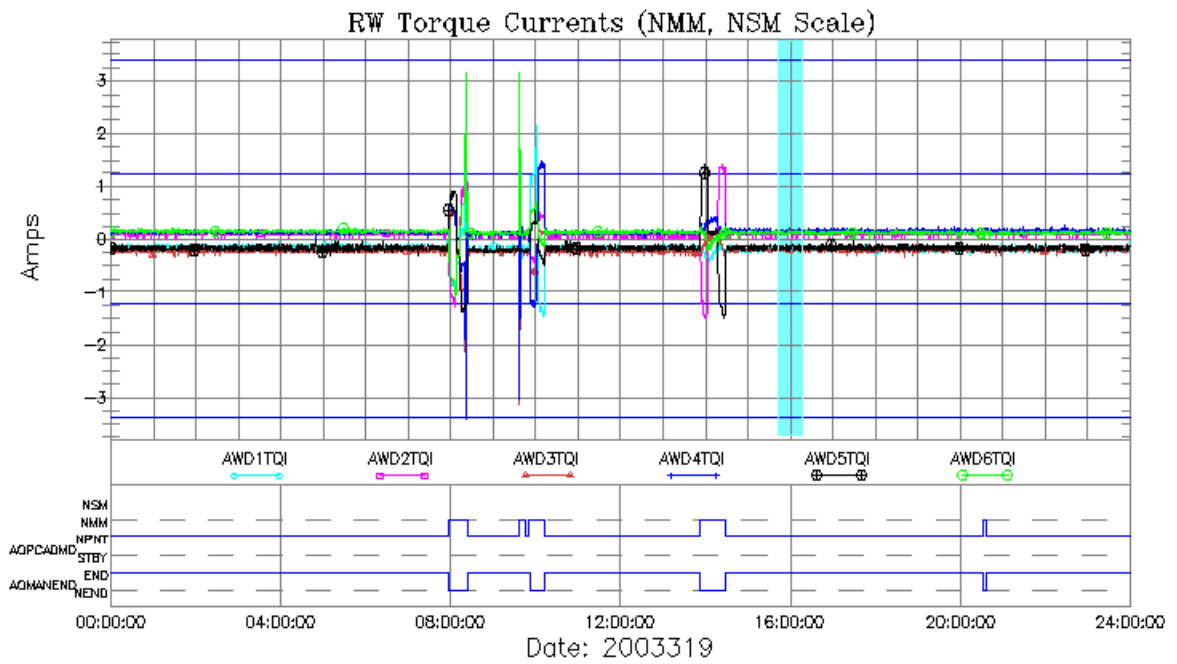
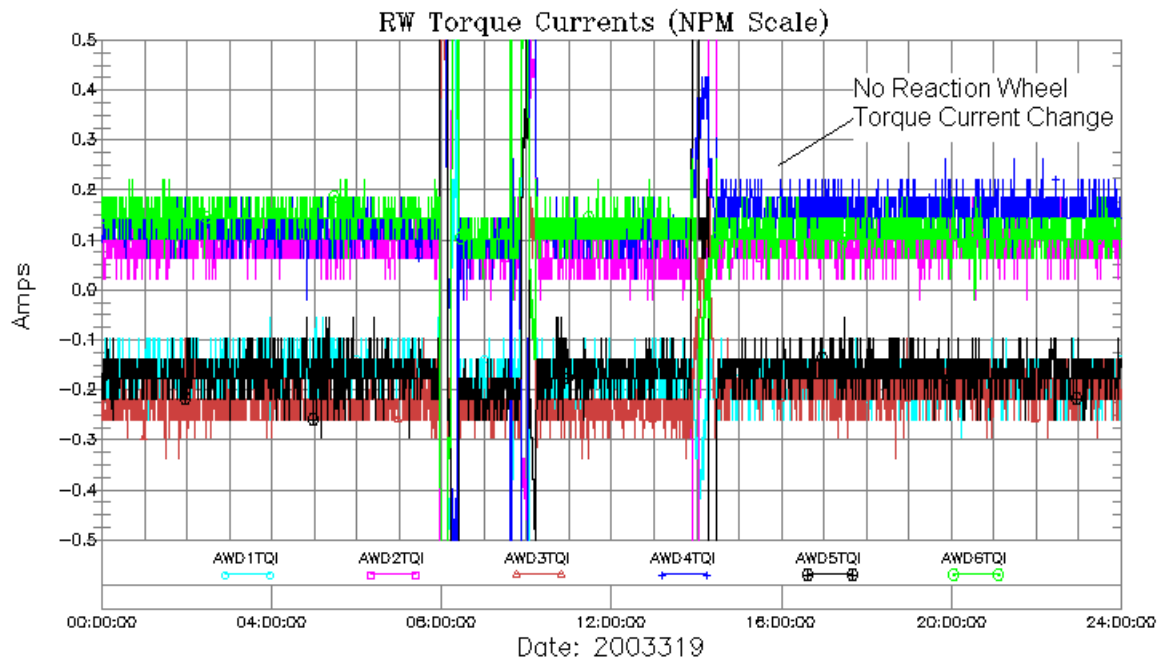


Figure 7: Reaction Wheel Torque Currents

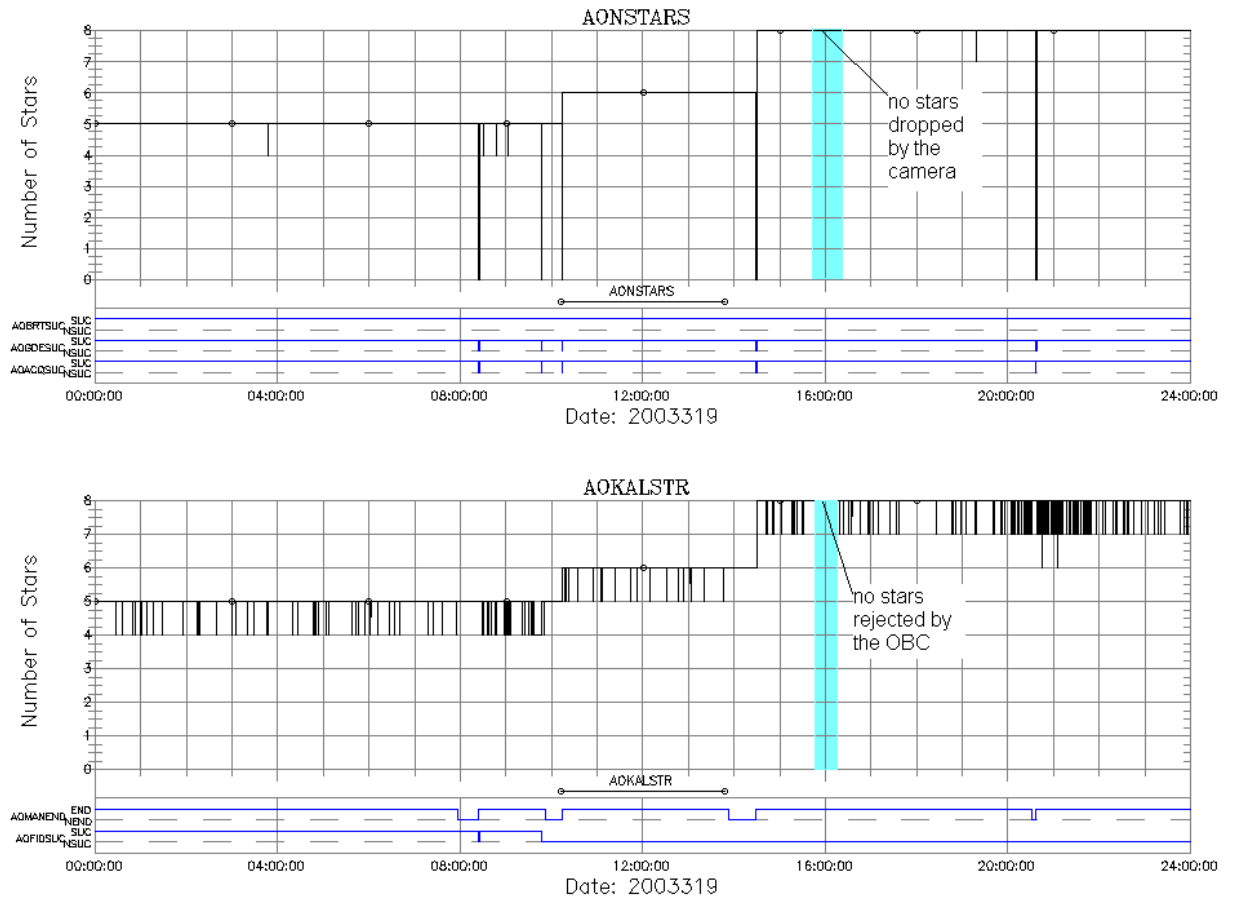


Figure 8: Number of Stars (Camera and OBC)

Once the daily plots were checked and the usual explanations (in terms of anticipated or unanticipated spacecraft commanding) were ruled out, a more thorough investigation of the telemetry was required. First, the top level PCAD health and status GRETA display (EHS_A_1NOC.dec) was played back for the time period and checked for any unusual behavior. None was found. A plot of the spacecraft rates and attitude errors was used to establish a time and size for the observed disturbance (**Figure 9**). The disturbance occurred at 2003:319:15:54:43 and had a magnitude of approximately 13 arcsec. Along with the rate, the disturbance torque, which is the input to the spacecraft momentum monitor that compares the expected change in momentum from thruster firings to the observed change in the momentum, was checked (**Figure 10**). The disturbance was noticeable, but far too small to trip the spacecraft momentum monitor.

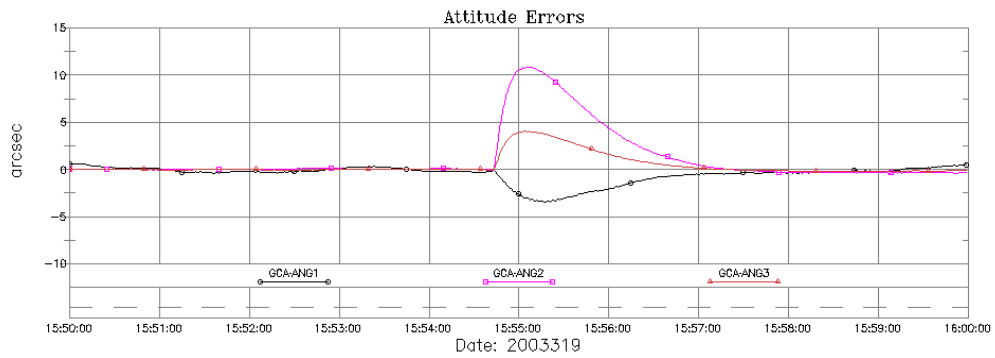
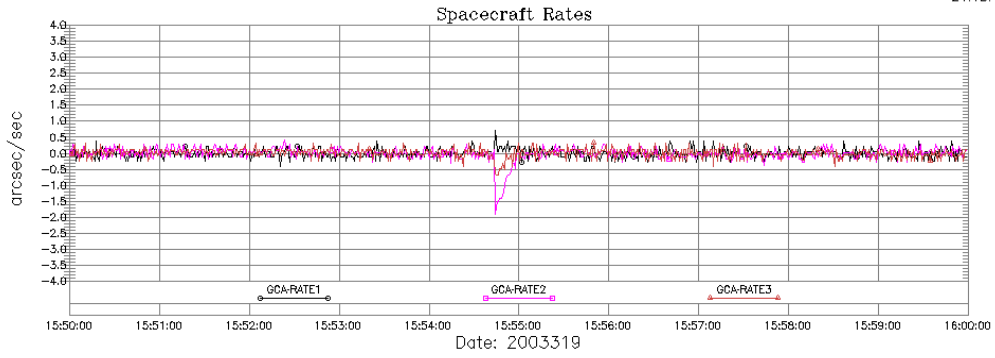


Figure 9: Spacecraft Rates and Attitude Error

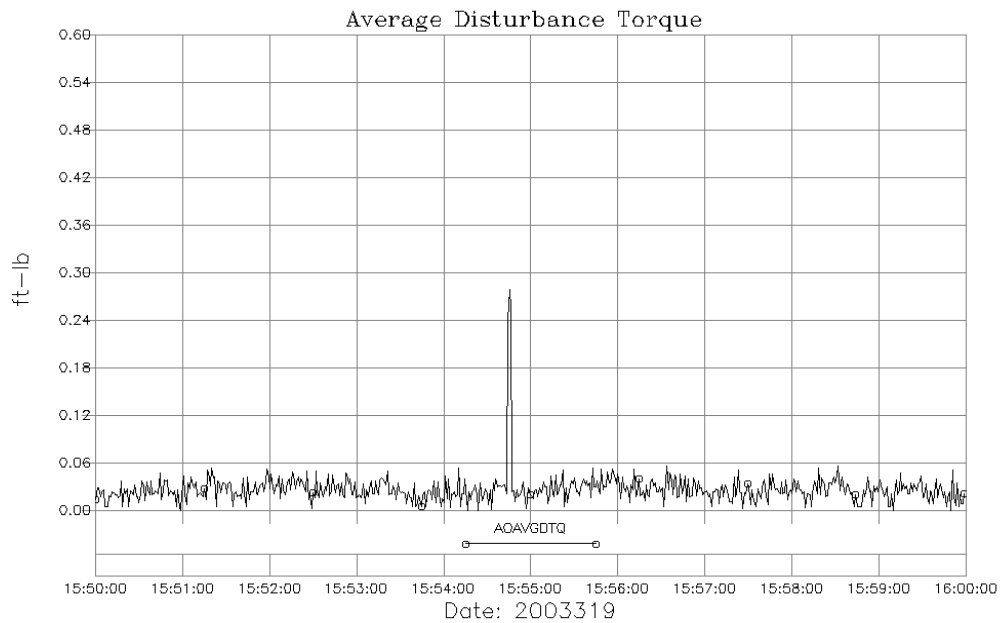


Figure 10: Disturbance torque

Fault Tree Analysis:

Once the weekly loads and safing actions were exonerated and the disturbance was characterized a systematic fault investigation was started. The items investigated are shown in **Figure 11**.

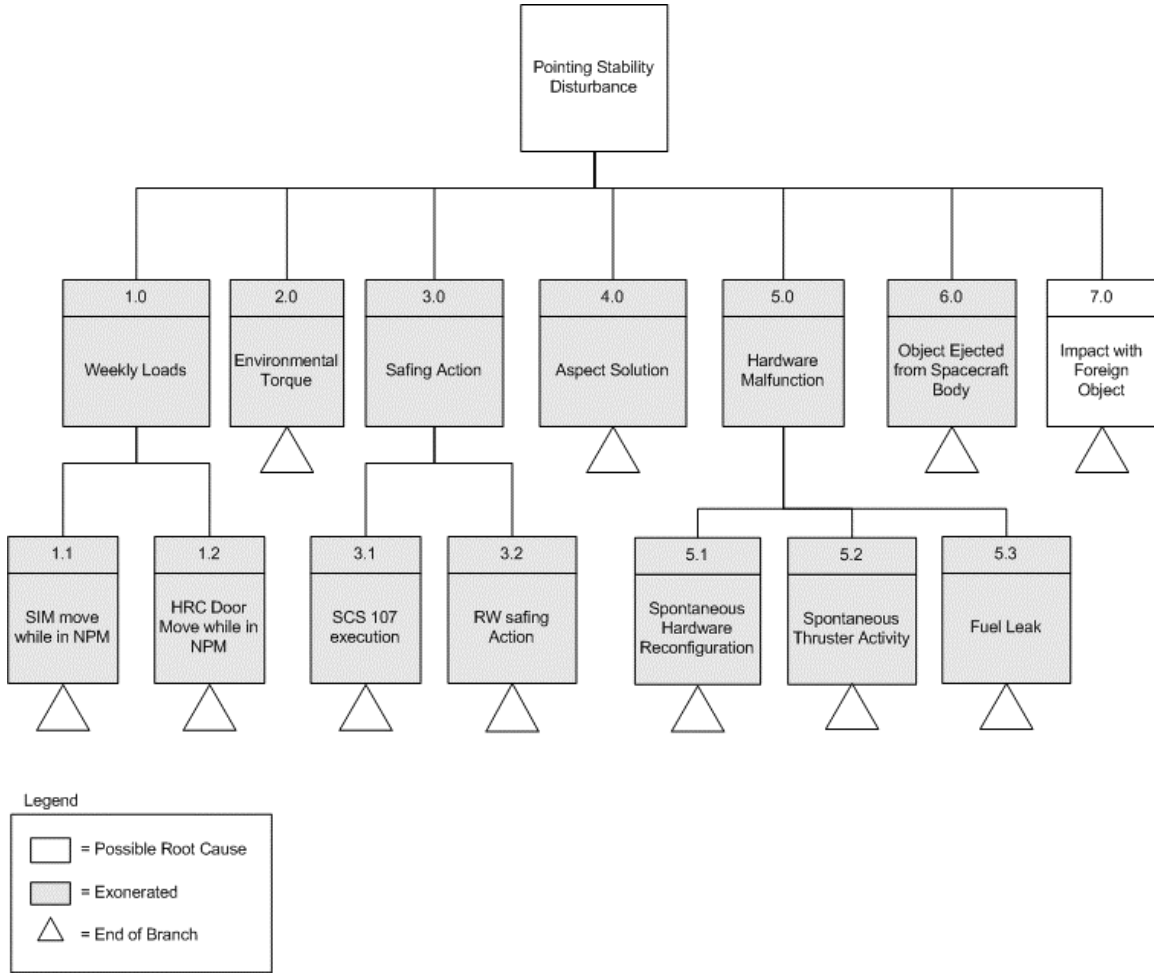


Figure 11: 2003:319 Attitude Disturbance Fault Tree

1.0 Weekly Loads (Exonerated)

Mechanism moves commanded in the weekly loads can cause disturbances in the pointing stability similar to the one observed on 2003:319.

1.1 SIM move while in Normal Pointing Mode (Exonerated)

When safing for the Radiation Zone the SIM is moved to the HRC-S position. Due to relative timing of the SIM move and the maneuver to the ACIS CTI attitude, this SIM move occasionally occurs while the spacecraft is in Normal Pointing Mode. A SIM move while in NPM will cause a large disturbance in the pointing stability. The weekly loads were checked and there was no commanding within one hour of the disturbance.

1.2 HRC Door Move while in Normal Pointing Mode (Exonerated)

Due to relative timing of maneuvers and Science Instrument setup, the HRC Door is occasionally moved while the spacecraft is in NPM. This will cause a disturbance in the pointing stability. The weekly loads were checked and there was no commanding within one hour of the disturbance.

2.0 Environmental Torques (Exonerated)

Environmental torques change gradually as the relative positions of the spacecraft, the Earth and the Sun change. Errors produced by an environmental torque would be gradual and persistent, not instantaneous and transient as occurred during the disturbance of 2003:319.

3.0 Safing Actions (Exonerated)

Any safing action that moves the SIM, commands the HRC Door or impacts the reaction wheels could cause a pointing stability disturbance.

3.1 SCS 107 Execution (Exonerated)

SCS 107 moves the SIM to the mid-point and then to HRC-S all while the spacecraft is in NPM. This creates a large disturbance in the pointing stability plot. SCS 107 was inactive after the disturbance of 2003:319 and not disabled as it would be had it executed. Also, none of the expected errors or limit violations associated with an SCS 107 execution were present at the time of the disturbance. Finally, the spacecraft weekly loads, which are terminated by SCS 107, were still executing.

3.2 RW Safing Action (Exonerated)

A problem with a reaction wheel would cause degraded pointing performance. The reaction wheel state of health plots showed no problems. Additionally, all of the reaction wheel safing actions (SCSs 17-22) were inactive, not disabled as they would be if one had executed. Finally, the reaction wheel safing actions take a wheel offline and disable the reaction wheel bias, but neither of these actions had taken place.

4.0 Aspect Solution (Exonerated)

Stray light in the Aspect Camera can cause an error in the aspect solution, which in turn can cause a spike in the on-board attitude error calculation. This would produce a disturbance in the pointing stability plot. Plots of star positions were used to determine the source of any possible error (**Figure 12**). Due to the nature of the disturbance, if it were caused by stray light in the camera, the source would have to be instantaneous, such as a cosmic ray. A cosmic ray would shift the centroid of only one star. If the attitude were perturbed (exonerating the camera), all of the stars would instantaneously shift in the same direction. The data supported the latter characterization of the event.

Ref: 5504256@2003312.211028
A-ACA-01-leo.dec
VCDU:2003319.000000-737680.ztlm

ACA IMAGES 0-1
Flight Data

Northrop Grumman/FOT
Generated Nov 17, 2003 (Day 321)
21:13:27 Z

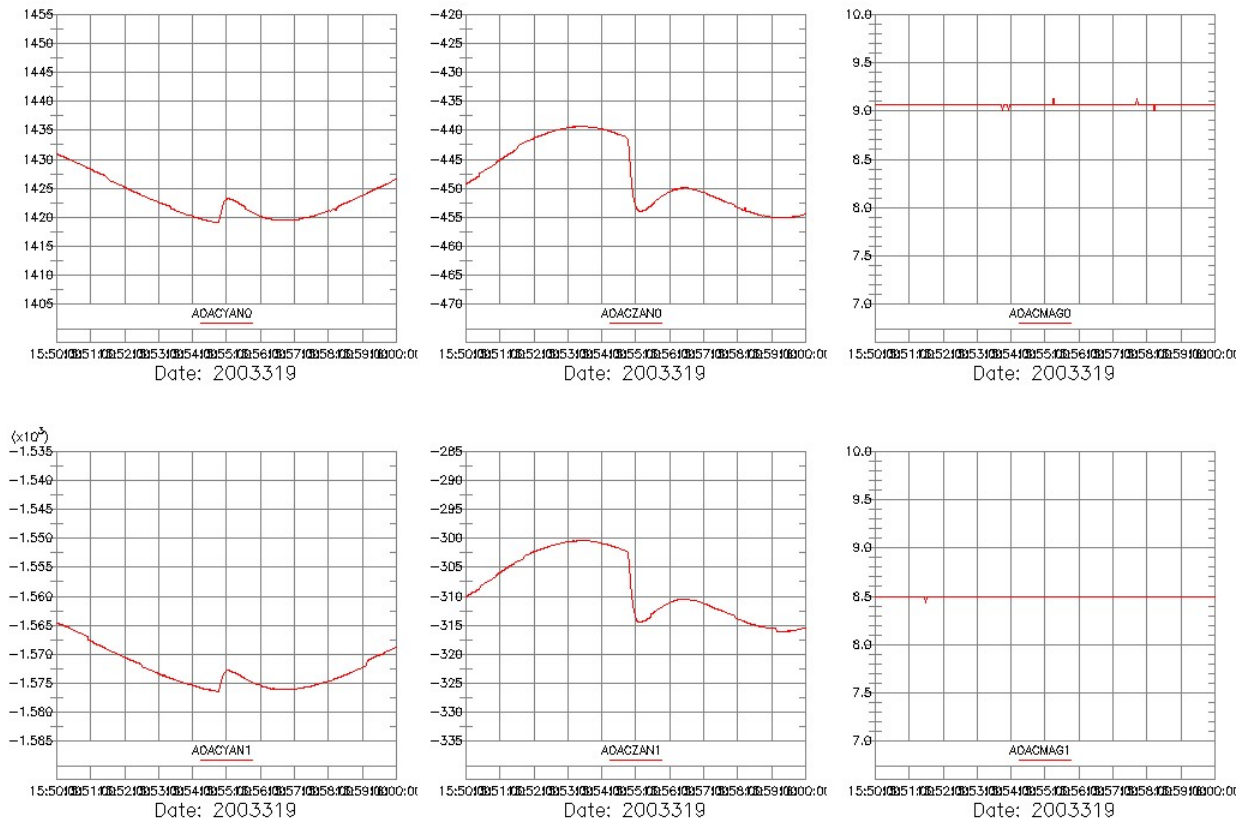


Figure 12: Star Positions (one of four)

5.0 Hardware Malfunction (Exonerated)

Some spontaneous hardware operations or reconfigurations could cause a spike in the pointing stability. A reconfiguration, such as a spontaneous mechanism move or a part detaching from its structure, would cause a redistribution of momentum. A spontaneous thruster firing or fuel leak would cause a change in the total system momentum. In order to further characterize the disturbance, the system momentum was checked.

The GRETA plot for system momentum showed no change at the time of the disturbance (**Figure 13**). However, the OBC only reports the telemetry for system momentum once every eight seconds. It was felt that an attitude error of thirteen arcsec would certainly cause some redistribution of momentum. Due to the MUPS anomaly, a tool that calculates the system momentum from the reaction wheel speeds and gyro counts had been developed. This tool provides system momentum on a quarter second time step. The tool was used to calculate the system momentum for the disturbance (**Figure 14**).

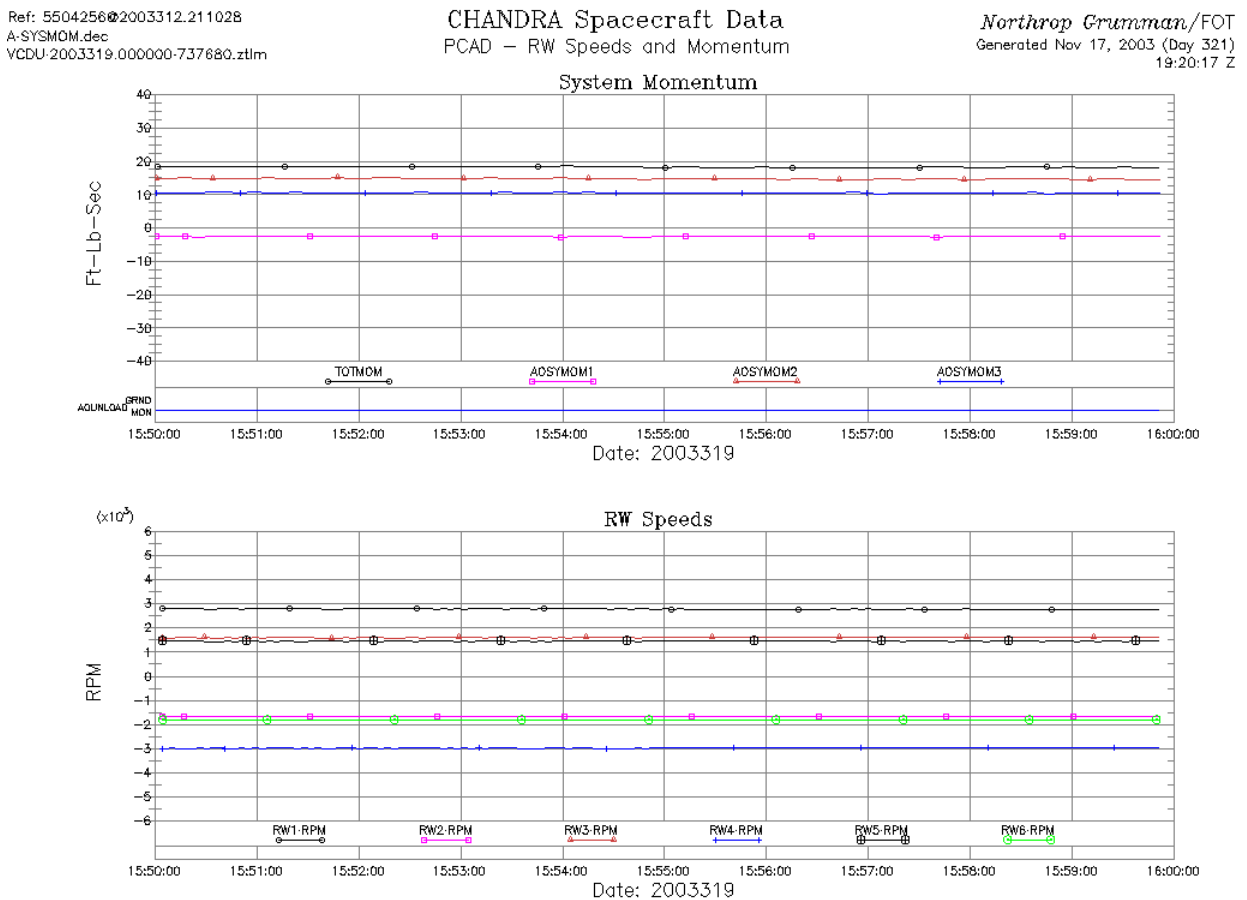


Figure 13: System Momentum GRETA display

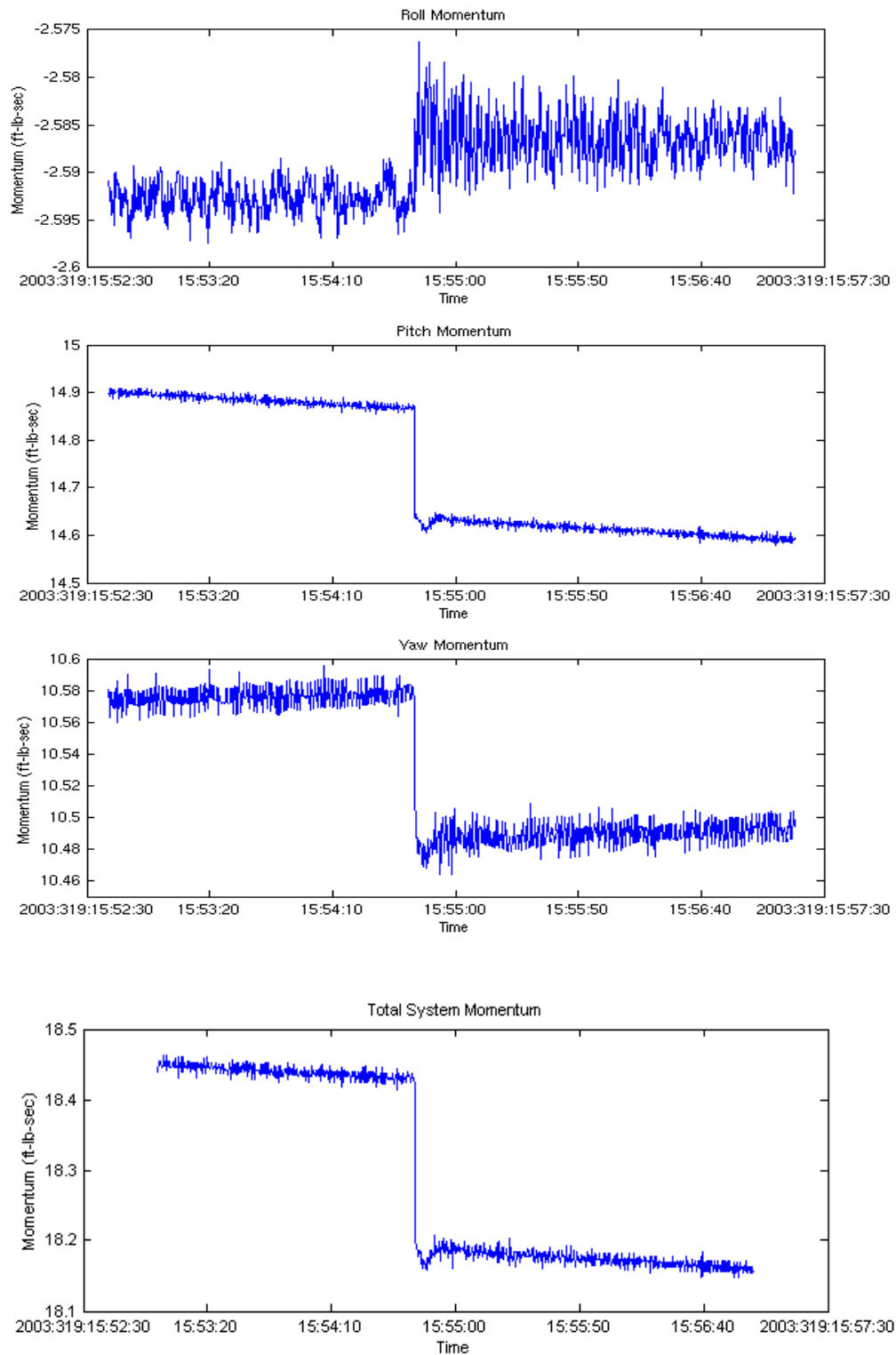


Figure 14: System Momentum Computed from RW and Gyro Data

5.1 *Spontaneous Hardware Reconfiguration* (Exonerated)

A hardware reconfiguration can cause the spacecraft momentum to redistribute itself among the spacecraft axes. Due to the conservation of momentum, a reconfiguration cannot create or dissipate momentum (the total system momentum remains unchanged). Figure 14 shows that the disturbance changed the total system momentum, so it cannot be due to a spontaneous hardware reconfiguration.

5.2 *Spontaneous Thruster Activity* (Exonerated)

While a hardware reconfiguration cannot create momentum, the MUPS thrusters are designed to change the system momentum. A spurious firing of one of the MUPS thrusters could cause a disturbance such as the one seen on 2003:319. Therefore, the Propulsion telemetry was checked carefully. The Valve Drive Electronics (VDE) was not activated, there was no firing heat signature at any of the thruster valves, no change in temperature on any of the propulsion line thermistors and no change in tank pressures. The telemetry for the thruster state of health procedure was checked and the magnitude of the disturbance would correspond to a 20 ms pulse on a MUPS thruster. The propulsion telemetry showed no evidence of anomalous behavior, but the fidelity of the telemetry is insufficient to analyze thruster activity at the 20 ms pulse level. The lack of fidelity in telemetry did not allow completely ruling out spurious thruster activity through hardware telemetry alone. However, the force from a given thruster has a definite and well-known direction. A single MUPS thruster has the most control authority in pitch, then roll, then yaw. So a single MUPS firing should produce the largest change in pitch, followed by roll, with the smallest change in yaw. This is not what the telemetry shows. The change in roll is far smaller than the change in pitch or yaw, so qualitatively the momentum change could not have been due to a MUPS thruster. A more quantitative answer was provided by using the MUPS thruster calibration to calculate the thrusters required to produce the observed change in momentum. It was found that three MUPS thrusters would have to fire spontaneously and simultaneously to produce the observed change in momentum. Thus it was concluded that a spurious MUPS thruster firing could not have caused the attitude disturbance of 2003:319. The RCS thrusters and the LAEs were de-activated after OAC, so they were not considered in the assessment of probable cause.

5.3 *Fuel Leak* (Exonerated)

The check of the propulsion subsystem telemetry included a check of line temperatures and tank pressures. A fuel leak would likely cause a temperature drop in the line with the leak. There was no change in the line temperatures near the time of the attitude disturbance. A leak would also cause a gradual change in tank pressure. The tank pressures have been steady since the attitude disturbance. Finally, a leak would cause a gradual change in the rate

of momentum accumulation, not an instantaneous change. If the attitude disturbance were due to a fuel leak, Figure 14 would show a change in slope, which it does not.

Impacting or Ejected Object: Analysis for Fault Tree Cases 6.0 and 7.0

The remaining two cases (6.0 and 7.0) involve an object being ejected from, or colliding with, the spacecraft body. Note that the most likely type of object that might collide with the spacecraft is a micrometeoroid, since Chandra is far outside the region near the Earth that contains debris.

It was known that day 319 was during the Leonid meteoroid storm. Mission Planning was consulted and it was determined that 2003:319:15:54 was during a period of elevated activity for the Leonids, though not during one of the peak activity periods, and that the spacecraft was not shielded from the Leonids by the Earth at that time. At the same time, however, the so-called Northern Apex source of sporadic meteoroids was ~ 10 deg away from the Leonid radiant. The flux of these apex source meteoroids was at least an order of magnitude larger than the Leonid flux at the time of the attitude disturbance event (Bill Cooke, private communication).

In order to evaluate these cases, we can calculate rough estimates for the mass of a particle that could produce the observed change in angular momentum.

Relating the change in angular momentum of the spacecraft body, $\Delta\mathbf{H}$, to the mass of the particle, Δm , we have:

$$\Delta\mathbf{H} = \mathbf{r} \times \Delta\mathbf{p} = \mathbf{r} \times (\Delta m \cdot \mathbf{v}) = \Delta m (\mathbf{r} \times \mathbf{v})$$

where

- \mathbf{r} = position vector of particle impact/ejection site
(relative to body center of mass)
- $\Delta\mathbf{p}$ = momentum added to body by impact/ejection
(assumes completely inelastic collision in the impact case)
- \mathbf{v} = particle velocity

Then the magnitude of the change in angular momentum is:

$$|\Delta\mathbf{H}| = \Delta m \cdot r \cdot v \cdot \sin \theta$$

where

$$\theta = \text{angle between } \mathbf{r} \text{ and } \mathbf{v}.$$

A priori, θ is unknown, so assume $\sin \theta = 1$.

Now, the observed change in angular momentum was $|\Delta\mathbf{H}| = 0.33 \text{ N}\cdot\text{m}\cdot\text{s}$ in the body frame of reference, so:

$$\Delta m \sim |\Delta\mathbf{H}| / (r \cdot v)$$

(Note that subsequent calculations in this section are also done in the body frame.)

The end of the Sun Shade Door (SSD) is about 4 m from the spacecraft center of mass (CM) and the SIM is about 8 m away from the CM.

The mean speed for meteoroids relative to the Earth is about 20 km/s, while the speed of a Leonid meteoroid is about 75 km/s. The speed for an apex source sporadic meteoroid is about 55 km/s.

Consider several cases to get an impacting particle mass estimate:

	4 m	8 m
20 km/s	4.1 mg	2.1 mg
55 km/s	1.5 mg	0.8 mg
75 km/s	1.1 mg	0.6 mg

So a rough estimate of the mass of an impacting particle is $\sim 1 \text{ mg}$. A typical meteoroid density is $\sim 1 \text{ g/cm}^3$, which gives a particle diameter of $\sim 1 \text{ mm}$.

For a similar estimate for the mass of a piece of the spacecraft ejected from the body, we can use $r \sim 4 \text{ m}$ and $v \sim 1 \text{ m/s}$. These should be typical values and they give a rough mass estimate of $\sim 100 \text{ g}$.

Based on the mass estimates for an impacting or ejected object we can estimate the (linear) kinetic energy deposited in or removed from the spacecraft. This gives a measure of the damage potential of the event. For comparison, the kinetic energy of a fast baseball is $\sim 120 \text{ J}$ and that of a 0.22 caliber bullet is $\sim 136 \text{ J}$.

If we assume an impacting Leonid meteoroid with $r \sim 4 \text{ m}$, we find the added kinetic energy to be:

$$\Delta T_{\text{lin}} = (1/2) \Delta m \cdot v^2 \sim 3000 \text{ J}$$

An apex source meteoroid ($v = 55 \text{ km/s}$) gives $\Delta T_{\text{lin}} \sim 2300 \text{ J}$, while a more typical meteoroid ($v = 20 \text{ km/s}$) gives $\Delta T_{\text{lin}} \sim 800 \text{ J}$. Therefore, an impacting meteoroid will impart a few thousand Joules of kinetic energy to the spacecraft.

Compare these numbers to what would be expected from an ejected piece of the spacecraft, namely $\Delta T_{\text{lin}} \sim 0.05 \text{ J}$.

Next we estimate the additional rotational kinetic energy imparted to the spacecraft by this event.

$$\Delta T_{\text{rot}} = (1/2) \Delta \boldsymbol{\omega} \cdot \mathbf{I} \cdot \Delta \boldsymbol{\omega}$$

$$\Delta \mathbf{H} = \mathbf{I} \cdot \Delta \boldsymbol{\omega}$$

where

\mathbf{I} = spacecraft inertia tensor
 $\Delta \boldsymbol{\omega}$ = change in rotation rate

Using matrix notation, we have:

$$\Delta \mathbf{H} = \mathbf{I} \cdot \Delta \boldsymbol{\omega} \Rightarrow \Delta \boldsymbol{\omega} = \mathbf{I}^{-1} \cdot \Delta \mathbf{H}$$

$$\Delta T_{\text{rot}} = (1/2) \Delta \boldsymbol{\omega}^T (\mathbf{I} \cdot \Delta \boldsymbol{\omega}) = (1/2) \Delta \boldsymbol{\omega}^T \cdot \Delta \mathbf{H} = (1/2) (\mathbf{I}^{-1} \cdot \Delta \mathbf{H})^T \cdot \Delta \mathbf{H}$$

Now:

$$\Delta \mathbf{H} = \begin{pmatrix} 0.01 \\ -0.31 \\ -0.12 \end{pmatrix} \text{ N-m-s}$$

$$\mathbf{I} = \begin{pmatrix} 9106.392 & 57.672 & -828.570 \\ 57.672 & 49664.395 & 203.012 \\ -828.570 & 203.012 & 52838.429 \end{pmatrix} \text{ kg-m}^2$$

so we find $\Delta T_{\text{rot}} \sim 1 \times 10^{-6} \text{ J}$, which is negligible compared to ΔT_{lin} . Note that rotational kinematic effects due to an impacting or ejected object are the only ones that can be detected directly by sensors onboard the spacecraft.

As a simple check of the consistency of our results, we can calculate the expected change in rotation rate ($\Delta \boldsymbol{\omega} = \mathbf{I}^{-1} \cdot \Delta \mathbf{H}$):

$$\Delta \boldsymbol{\omega} = \begin{pmatrix} 0.19 \\ -1.29 \\ -0.46 \end{pmatrix} \text{ arcsec/s}$$

This compares well to the measured angular rate change of:

$$\Delta\omega = \begin{pmatrix} 0.220 \\ -1.339 \\ -0.318 \end{pmatrix} \text{ arcsec/s}$$

6.0 Object Ejected from Spacecraft Body (Exonerated)

Based on the preceding analysis, an object ejected from the spacecraft is estimated to have a mass on the order of 0.1 kg and would be a significant component of the spacecraft. No evidence exists that such a piece of hardware has been lost.

7.0 Impact with a Foreign Object (Most Probable Root Cause)

Analysis shows that an impacting object, most likely a micrometeoroid, is estimated to have a mass on the order of 1 mg. This is within the range of meteoroid masses, but toward the high end. Such a particle definitely has the potential to cause damage to the spacecraft though no such damage has been found (see below).

The direction of the delta momentum vector at the time of the event was (see analysis below):

$$\begin{aligned} \text{RA} &= 276.4 \text{ deg} \\ \text{Dec} &= 37.1 \text{ deg} \end{aligned}$$

The Leonid radiant is at RA = 153 deg, Dec = 22 deg, and the apex source direction is RA = 144 deg, Dec = 29 deg. These two directions are about 10 deg apart and are both 100 deg away from the delta momentum vector direction.

An impact from the direction of the Leonids or the apex source could easily produce the observed change in momentum. Since the remaining root cause was impact by a foreign object and since the impact was during the Leonids period, it was determined that the most probable cause was an impact by a Leonid or other micrometeoroid.

Analysis of Impact Region:

Once the most probable root cause had been identified, the investigation was re-focused on identifying probable impact regions. Mission Planning contacted the Marshall Space Flight Center (MSFC) point of contact for Leonid planning, Bill Cooke. He indicated that the majority of the energy from a micrometeoroid impact would go into vaporizing the particle and that the collision could be considered inelastic. In an inelastic collision, the change in momentum must be normal to the moment arm. Therefore, the vector from the vehicle center of mass to the impact location must be normal to the delta momentum vector. This means that the analysis of the impact location hinges on an accurate calculation of the delta momentum.

Detailed Delta Momentum Analysis

Since analysis of the impact region was going to hinge on the delta momentum vector, great care was taken to find the best possible estimate of the change in momentum. The following method was used to compute the delta momentum:

1. Use Inertial Frame to remove effect of attitude perturbation
Use a Matlab function derived from Thruster Efficiency momentum calculation to compute system momentum in inertial frame. Function uses gyro counts, gyro bias, RW speeds (linear interpolation from 2 sec to quarter sec step) and on-board K-constants to compute momentum in body frame. Function then uses OBC estimated quaternion to rotate into Inertial frame.
2. Find t_0 .
Plot System Momentum in Inertial frame for impact time plus and minus 5 minutes versus point number index. Zoom on plot to determine index of last point before step change. Assign this index to be t_{0i} (time zero index). Then use t_{0i} to find the timestamp for t_0 .
3. Create indices for before, during and after event:
 b_i (before index) = 2 minutes ending 5 sec before t_0 .
 t_i (transient index) = 5 seconds before to 30 seconds after t_0 .
 a_i (after index) = 2 minutes starting 30 seconds after t_0 .
4. Find linear fits.
Find linear fit for inertial frame system momentum for each axis (Roll, Pitch, Yaw) for both b_i and a_i . Use $x=(\text{timestamp}-t_0)$, $y=\text{sysmom}(\text{axis})$.
5. Check quadratic fit.
Repeat the fits using a quadratic instead of a linear fit. Check the coefficient on the quadratic term. In this case the largest term was 4 orders of magnitude smaller than the linear term, so linear is sufficient.

6. Use linear equations to find delta momentum.
The fits have their intercepts at t_0 , so the delta momentum for each axis is the difference of the intercepts of the fits from before and after t_0 . In this instance: Roll = 0.022, Pitch = -0.197, Yaw = 0.150
7. Check mean of residuals
In this case the mean of the residuals was on the order of 10^{-14} .
8. Estimate Error.
Take the standard deviation of the residuals as the one sigma error. In this instance: Roll = 0.0074, Pitch = 0.0076, Yaw = 0.0057

The results are plotted in Figures 15-17.

Using this method:

The computed delta momentum is: [0.0222, -0.197, 0.150] ft-lb-s

The computed one sigma error is: [0.0074, 0.0076, 0.0057] ft-lb-s

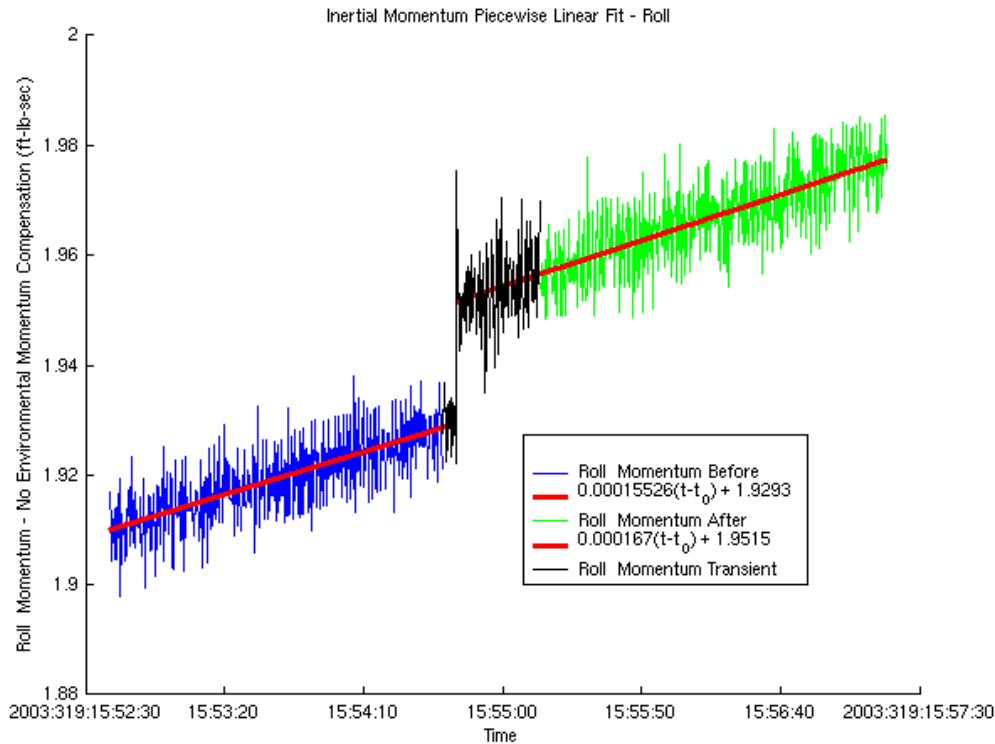


Figure 15: Roll Momentum for Disturbance of 2003319

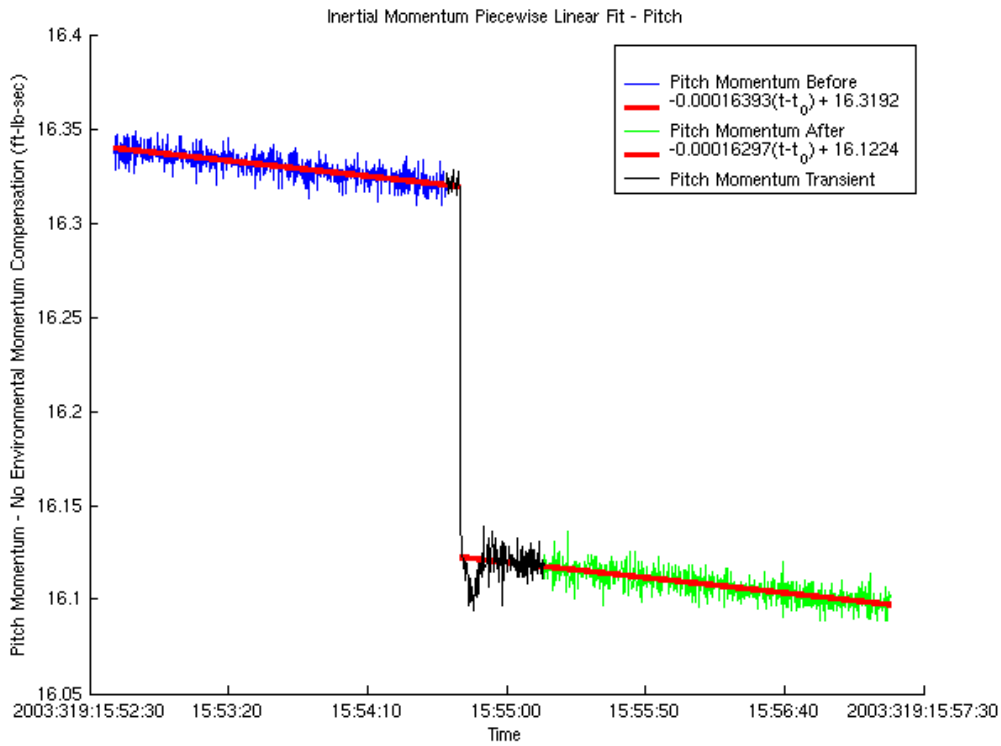


Figure 16: Pitch Momentum for Disturbance of 2003319

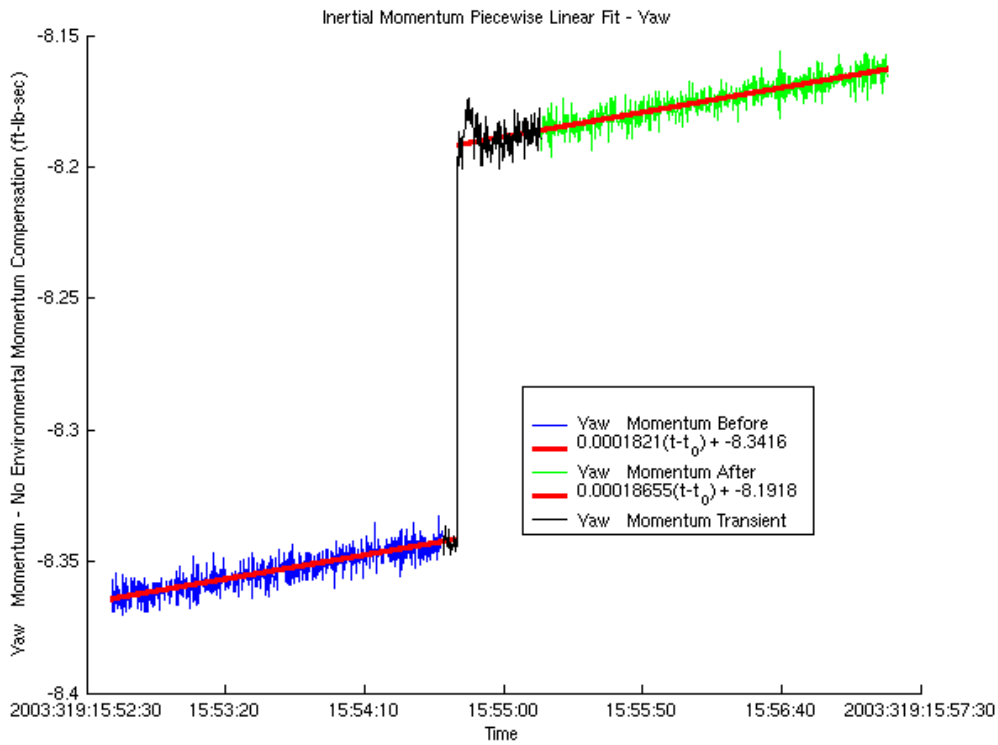


Figure 17: Yaw Momentum for Disturbance of 2003319

Satellite Tool Kit (STK) Analysis

Once an accurate delta momentum vector was found the analysis of possible impact region could start. STK is a valuable tool for this type of analysis; however, the accuracy of the model is vital to the accuracy of the analysis. To improve the model accuracy the center of mass of the vehicle was re-computed. This computation used the known positions of the MUPS thrusters and the torque calibration used in momentum analysis to compute the center of mass. The STK model was translated such that the center of the model was at the newly calculated center of mass. A comprehensive check of the model dimensions against the technical drawings provided by TRW was also completed. Once the model was updated and verified it could be used for impact region analysis. The analysis performed was as follows:

- Compute RA and Dec corresponding to ECI delta momentum using existing Matlab utilities (the result is RA \approx 276.4 deg, Dec \approx 37.1 deg)
- Add a star into the STK scenario at the computed RA and Dec of the momentum vector
- Add a 90° half-angle conic sensor targeted at the momentum “star” to create a plane normal to the delta momentum

Snapshots of the model with the possible impact plane are shown in **Figures 18 and 19**.

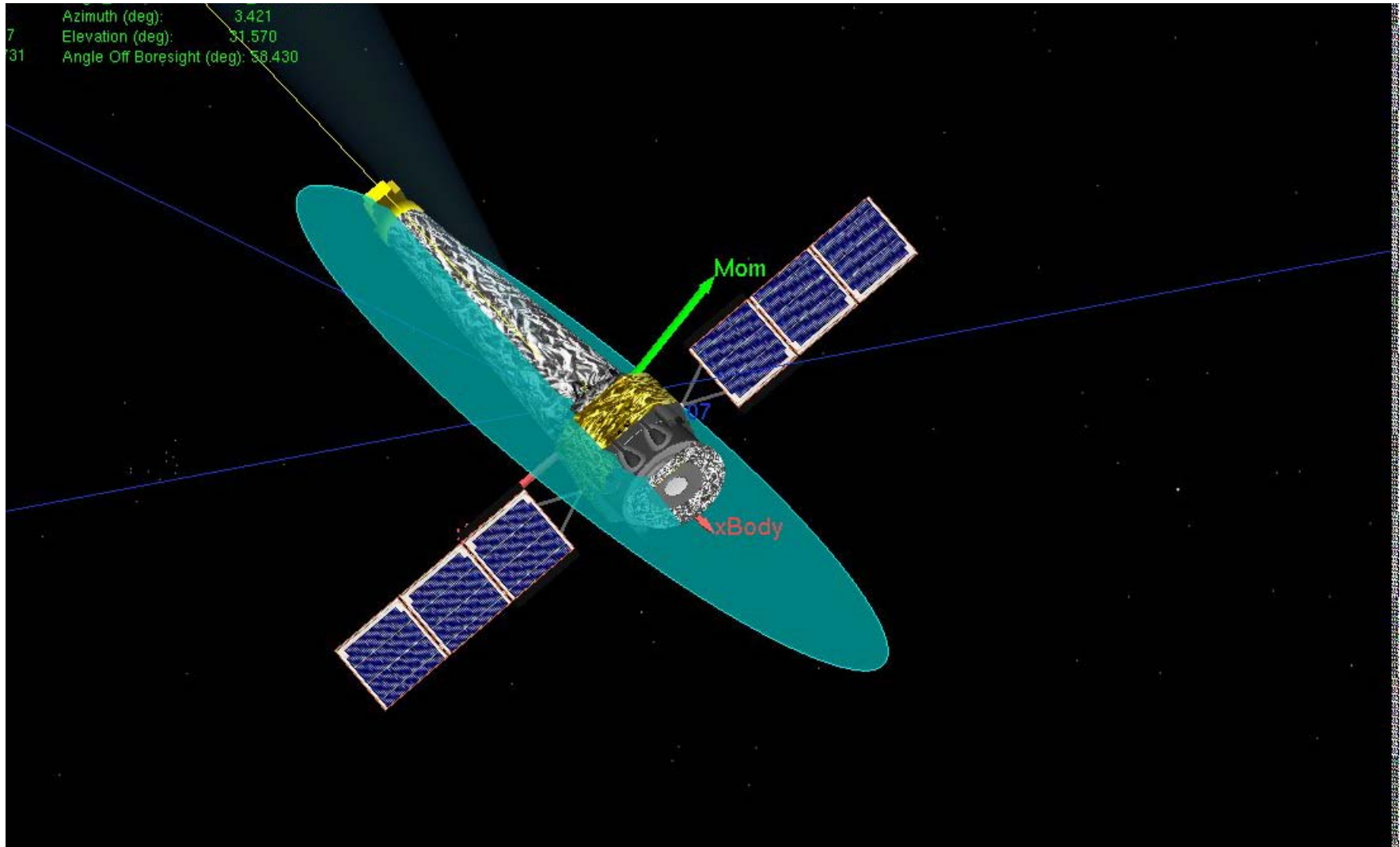


Figure 18: Plane Normal to Delta Momentum Vector

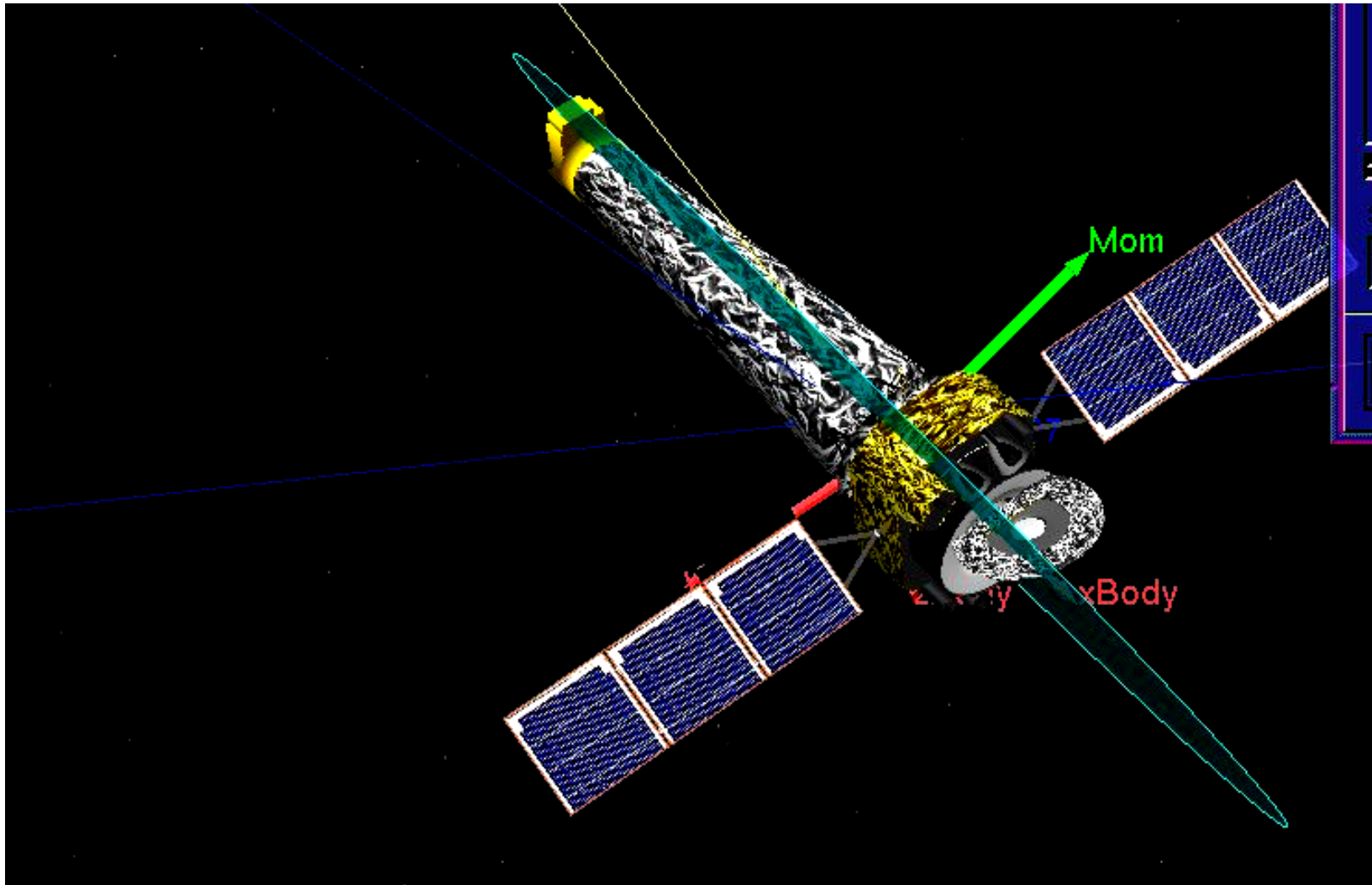


Figure 19: Plane normal to delta momentum vector

To better depict the possible impact region, the error in the momentum vector and its impact on the plane must be taken into account. The one sigma error computed in the delta momentum calculation was multiplied to give a three sigma error. The three sigma error was then used to form a box around the delta momentum vector. The angle between the delta momentum vector and each corner of the box was checked. The largest of these angles was taken as the error in the momentum vector and thus the plane. The largest angle was 2.75 degrees. The conic sensor depicting the plane was edited to have half angles of 87.25 and 92.75 degrees. This formed a swath through the spacecraft body. Any area inside of this swath is inside the potential impact region. Figures 20 to 23 show the swath.

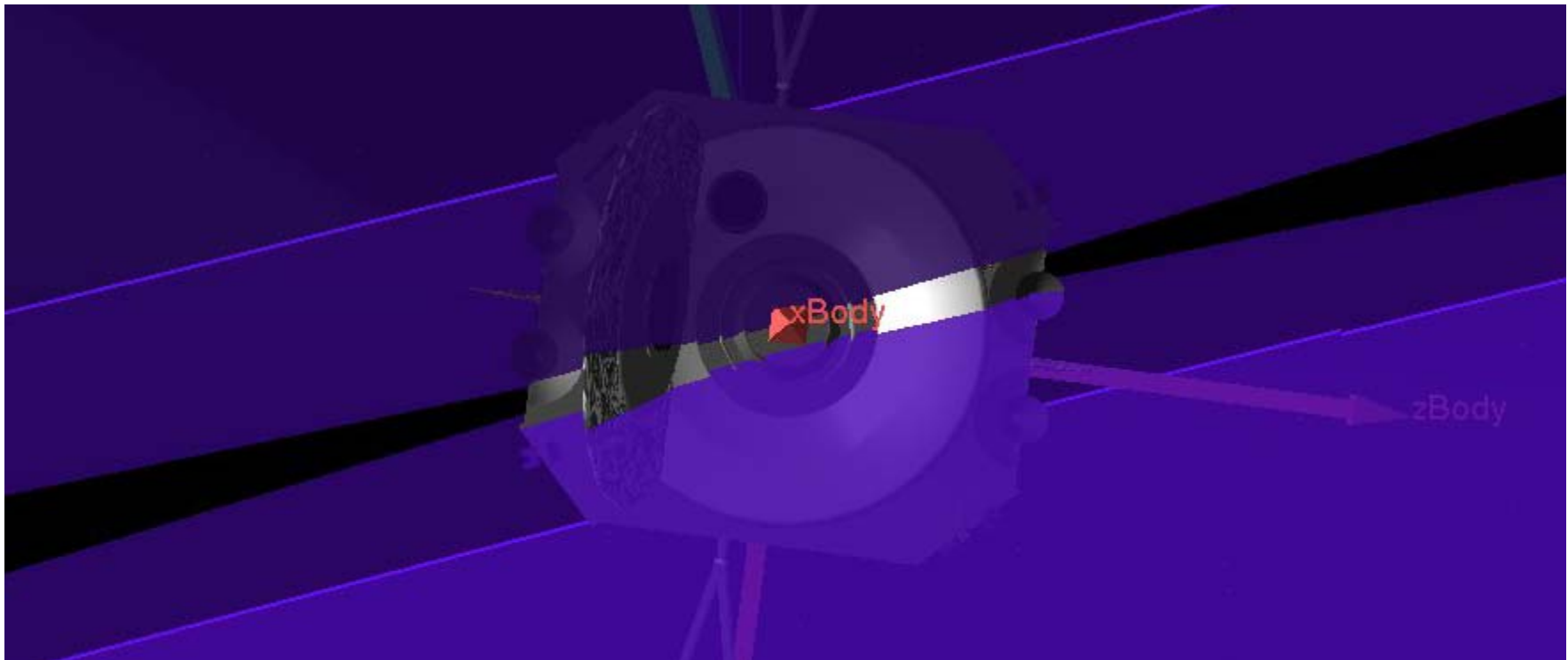


Figure 20: Possible Impact Region: +X view



Figure 21: Possible Impact Region: -Z view

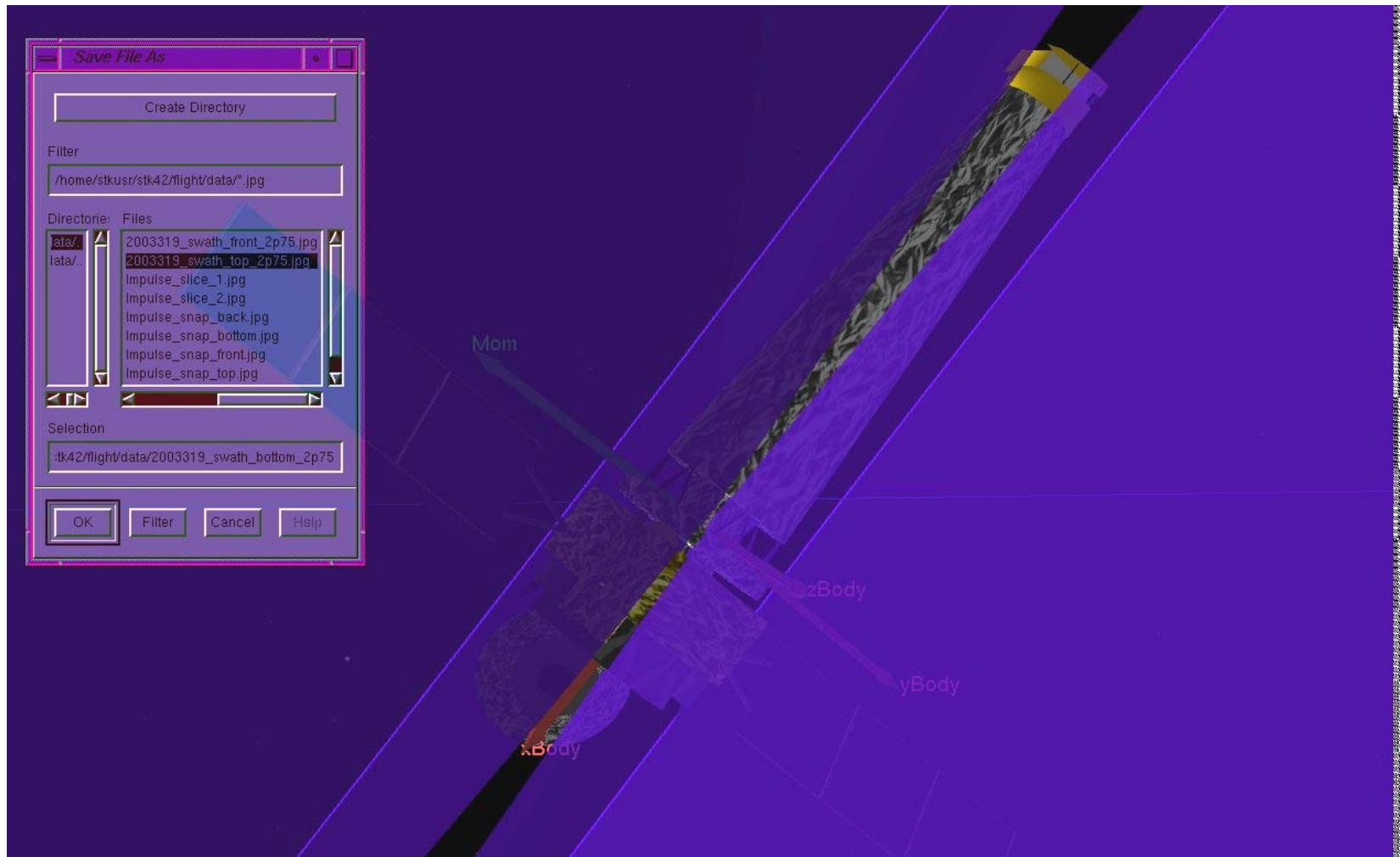


Figure 22: Possible Impact Region: +Z view

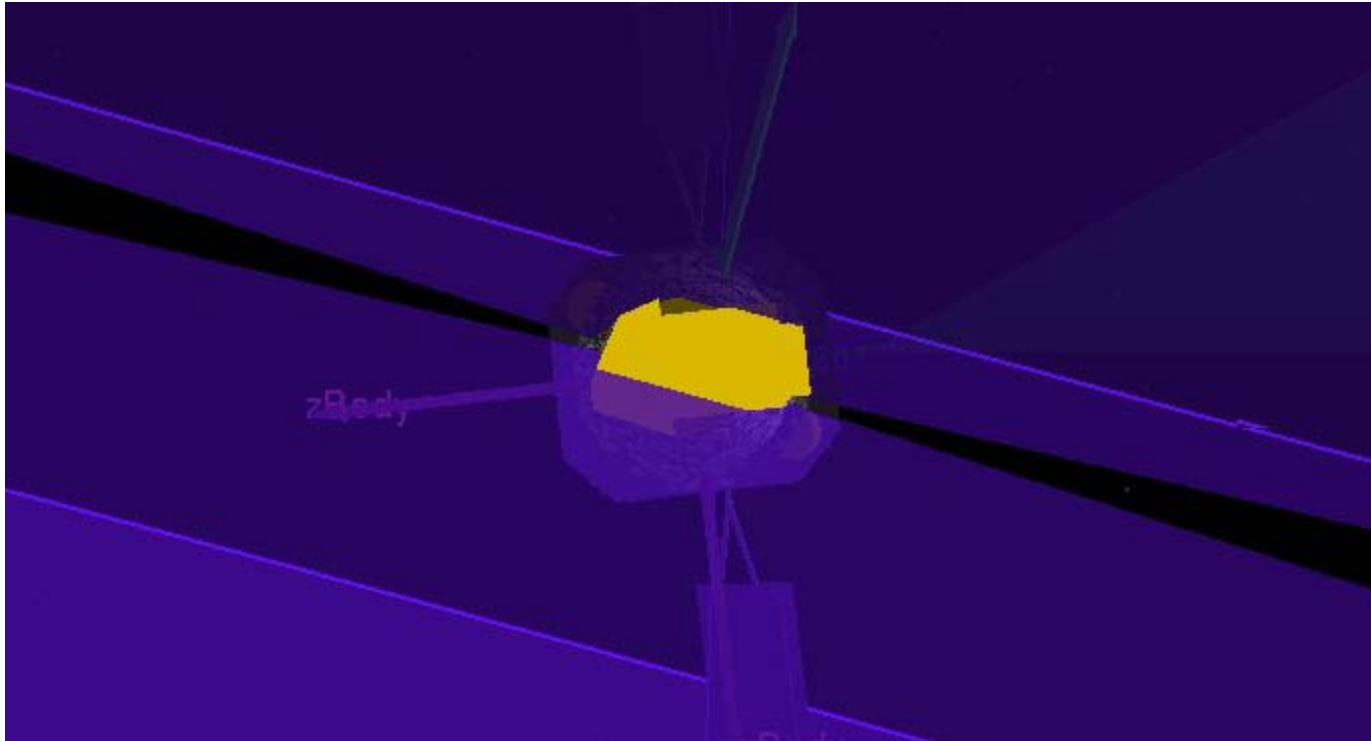


Figure 23: Possible Impact Region: -X view

Analysis of Surface Properties:

The system wide state of health check had shown that all of the primary units were functioning nominally. This could not however confirm the state of health of critical safing units, which are not nominally powered. The susceptibility of each of the core units and the control units was checked. It was found that the fine sun sensor and the MUPS thrusters were vulnerable to impact by a micrometeoroid. The core units and the redundant IRU were behind panels that protect them from such an impact. The impact region swaths show that neither the Fine Sun Sensor nor the MUPS are in the impact region. Therefore, state of health checks for the redundant units were determined to be unnecessary.

Once it was established that the top level spacecraft health and safety was not impacted by the event, the investigation focus changed yet again. The surface properties of the regions shown in Figures 20-23 were analyzed in hopes of better characterizing the impact.

The primary spacecraft health and safety concern regarding micrometeoroid impacts is due to plasma effects, which can cause electromagnetic interference with spacecraft systems. The Meteoroid Showers CARD (SYST-C-005) protects against plasma effects and no unusual behavior was detected at or near the time of the impact. Therefore, it was concluded that the spacecraft suffered no damage due to plasma effects.

The second concern is damage to spacecraft surfaces. Due to the uncertainties in the mass, velocity, density and shape of the incumbent particle and due to the effort required to find the material properties of each of the surfaces in the possible impact region, the damage equations derived for high velocity impacts cannot provide a reliable estimate of the likely damage to Chandra. Instead, documentation of the post-flight analysis of the surfaces of several spacecraft (EURECA, HST, LDEF) were reviewed. The documentation was searched for information on each of the surfaces listed in **Tables 1 and 2**. The information gained on each of the surface types and, when available, an image of the damage to that surface on one of the spacecraft listed above is provided in **Table 3**. **Table 4** lists any possible detection method for each surface, and if detection is possible lists the results of that analysis.

The following websites were used to collect spacecraft surface damage information:

Meteoroid Impacts:

http://www.estec.esa.nl/wmwww/wma/Collaborations/NoCDebris/Publications/met_2001_GD.pdf
<http://www.spennis.oma.be/spennis/help/background/metdeb/metdeb.html>

LDEF:

http://setas-www.larc.nasa.gov/LDEF/TECH_DISC/md.html

Olympus:

<http://www.selkirkshire.demon.co.uk/analoguesat/olympuspr.html>
http://arxiv.org/PS_cache/physics/pdf/9804/9804026.pdf

EURECA:
<http://esapub.esrin.esa.it/bulletin/bullet80/ace80.htm>
http://www.estec.esa.nl/wmwww/wma/R_and_D/eureca.html

HST:
http://www.estec.esa.nl/wmwww/wma/External/reports/gd/HST_OX_FR.doc
http://setas-www.larc.nasa.gov/HUBBLE/PRESENTATIONS/hubble_talk_humes_kinard.html

Table 1: Possible impact points forward of center of mass

Structure	Component	Surface	Substrate
-Z panel surface toward the +Y side	-Z panel	MLI-ST	GFRP facesheets over aluminum honeycomb
-Z panel +X surface toward the +Y side	-Z panel	MLI-ST	GFRP facesheets over aluminum honeycomb
LAE 4	Heat shield	titanium	
LAE 4	Thrust Chamber	Columbium (C-103), coated with Hitempco R512E silicide	
Thruster Tower		MLI-ST	GFRP
Spacecraft Central Cylinder -Z/+X, +Y side	Thermal Closeout	MLI-ST	GFRP facesheets over aluminum honeycomb
Sun Shade Door		MLI-ST	GFRP facesheets over aluminum honeycomb
Forward thermal closeout		Silver Teflon/ Kapton laminate	
Pre-collimator outside surface	HRMA	GFRP	
Propellant line bundles.	Below central cylinder thermal closeout.	Spiral -1 wrap	
Spacecraft Central Cylinder +Z/+X, -Y side	Thermal Closeout	MLI-ST	GFRP facesheets over aluminum honeycomb

Table 2: Possible impact points Aft of center of mass

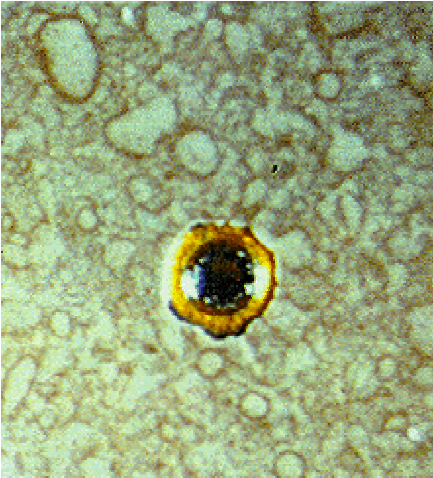
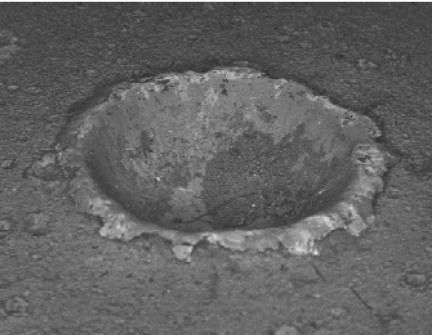
Structure	Component	Surface	Substrate
+Z panel surface toward the -Y side	+Z panel (Battery Compartment)	Kapton MLI & quartz mirror radiators	GFRP facesheets over aluminum honeycomb
+Z side of spacecraft to TFTE Aft Cylinder	Spacecraft to telescope interface	MLI-ST	GFRP facesheets over aluminum honeycomb
TFTE	Aft Cylinder structure	Stainless steel screen, MLI-ST, GFRP radiators	
+Z side of OBA	Optical Bench Assemble	MLI-ST	GRFP over aluminum honeycomb varying thicknesses
ISIM	Skirt	MLI-ST	GFRP facesheets over aluminum honeycomb
ISIM	ACIS Telescope Shade	MLI – 20 layer VDA Kapton Outer, VDA mylar inner layers with Dacron seperators	GFRP facesheets over fiberglass honeycomb
ISIM	Translation Table (+Z/+X side if HRC was in focal position)	Z93 white paint	GFRP facesheets over aluminum honeycomb
ISIM	ACIS Cold Radiator	Aluminum Plate, Martin Black paint.	
ISIM	ACIS Sun Shade	Goldized on interior, MLI-ST exterior	GFRP facesheets over fiberglass honeycomb
ISIM	-X Surface Turtle Shell	OSR's (Optical Solar Reflectors, quartz)	GFRP facesheets over aluminum honeycomb

MLI-ST = Multi layer insulation consisting of 24 layers. Outer layer 5 mil silver Teflon bonded to 2 mil aluminized kapton. Sub-layers are 0.33 mil double sided aluminized kapton with Dacron scrim cloth separators.

Spiral-1 = Multi layer insulation consisting of 12 layers. Outer layer 0.5 mil aluminized kapton. Sub-layers are 0.33 mil single sided aluminized kapton.

GRFP=Glass Fiber Reinforced Polymer

Table 3: Possible surface damage

Surface	Impact	Image
<p>MLI over GFRP facesheets</p>	<p>A study of micrometeoroid damage in the Eureka program post-flight analysis showed that the multi-layer insulation (MLI) structure retains particles up to a certain size very efficiently. Of 71 detected impacts only two penetrated the MLI. Any loss in thermal-control function due to the particle impacts was negligible. Study of the HST MLI blankets, similar to those used on Chandra, shows that each layer of insulation slows down and fractures the particle. There were no impacts that penetrated the MLI on HST.</p> <p>Were a particle to penetrate the MLI it would have been significantly slowed down and would likely have been fractured by its impact with each of the MLI layers. This (these) lower velocity, smaller mass particle(s) would not likely penetrate underlying GFRP facesheet.</p>	
<p>MLI over Spiral-1 wrap</p>	<p>See MLI.</p> <p>Were a particle to penetrate the first layer of MLI it would then have to penetrate the spiral wrap MLI before coming into contact with the propellant lines.</p>	<p>See MLI</p>
<p>GFRP</p>	<p>In the studies consulted no information could be found on the damage to GFRP caused by an incumbent particle. Further attempts to find information were unsuccessful. The only GFRP surface in the possible impact region not protected by MLI is the translation table. Due to the strength of the material it is thought to be highly unlikely that the particle would cause any significant damage.</p>	
<p>Titanium</p>	<p>The impact studies consulted only studied the impact on titanium fuel tanks. The image provided is that of a crater in a titanium fuel tank. There is no report of a fuel tank being compromised by an incumbent particle.</p>	


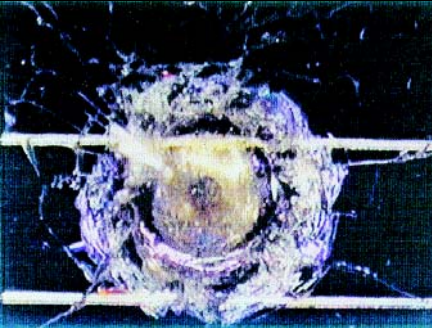
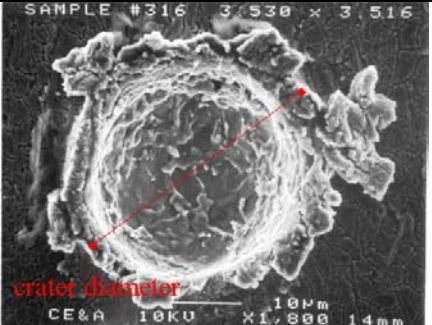
Surface	Impact	Image
Painted surfaces	The studies consulted showed that, when a painted surface is impacted by a micrometeoroid, a spall zone, shown right, is created. Any marring of the painted surfaces will decrease their reflective/absorptive properties, decreasing their thermal performance. The damage caused by such a spall zone is thought to be negligible when compared to the degradation from several years on orbit.	
OSRs (Optical Solar Reflectors, quartz)	There were no data provided on OSRs, but extensive information on damage to solar array cells is available. It is expected that the shattering of the cover glass seen in solar array cells would also be present if an OSR was impacted. This would decrease the impacted OSRs ability to reflect solar radiation, decreasing its functionality. It is not anticipated that damage to a single OSR will significantly impact the thermal protection provided by the set of OSRs.	
Aluminum Plate	The image at right shows a crater in an aluminum plate created by a small, high velocity particle. The size of the crater is dependant on the incumbent particle's mass and velocity. Were the incumbent particle to have enough mass and velocity the particle can, and has been seen to, penetrate the plate.	

Table 4: Detection Methods and Results

Structure	Component	Detection Method	Damage Detected
-Z panel surface toward the +Y side	-Z panel	Any loss in MLI thermal-control function due to particle impacts is thought to be negligible, so detection is not possible.	N/A
-Z panel +X surface toward the +Y side	-Z panel	Any loss in MLI thermal-control function due to particle impacts is thought to be negligible, so detection is not possible.	N/A
LAE 4, heat shield	Heat shield	The heat shield does not have any instrumentation of its own and is no longer operationally used, so no detection is possible.	N/A
LAE 4	Thrust Chamber	Were the thrust chamber compromised the most likely detection method would be firing. Since the LAEs have been deactivated detection is not possible.	N/A
Thruster Tower		The thruster tower is protected by MLI and GFRP facesheets. Any loss in MLI thermal-control function due to particle impacts is thought to be negligible, so detection is not possible.	N/A
Spacecraft Central Cylinder -Z/+X, +Y side	Thermal Closeout	Any loss in MLI thermal-control function due to particle impacts is thought to be negligible, so detection is not possible.	N/A
Sun Shade Door		The Sun Shade Door has no instrumentation, so detection is not possible.	N/A
Forward thermal closeout		Any loss in MLI thermal-control function due to particle impacts is thought to be negligible, so detection is not possible.	N/A
Pre-collimator outside surface	HRMA	Any loss in thermal-control function due to particle impacts is thought to be negligible, so detection is not possible.	N/A
Propellant line bundles.	Below central cylinder thermal closeout.	Any loss in MLI thermal-control function due to particle impacts is thought to be negligible, so an impact to the MLI is not detectable. Were a particle to penetrate the spiral wrap and puncture a propellant line there would be a fuel leak. This would be detectable in tank pressures and momentum accumulation following the event.	None. There was no change in tank pressures or momentum accumulation following the event.

Structure	Component	Detection Method	Damage Detected
Spacecraft Central Cylinder +Z/+X, -Y side	Thermal Closeout	Any loss in MLI thermal-control function due to particle impacts is thought to be negligible, so detection is not possible.	N/A
+Z panel surface toward the -Y side	+Z panel (Battery Compartment)	Any loss in MLI thermal-control function due to particle impacts is thought to be negligible, so detection is not possible.	N/A
+Z side of spacecraft to TFTE Aft Cylinder	Spacecraft to telescope interface	Any loss in MLI thermal-control function due to particle impacts is thought to be negligible, so detection is not possible.	N/A
TFTE	Aft Cylinder structure	Any loss in MLI thermal-control function due to particle impacts is thought to be negligible, so detection is not possible.	N/A
+Z side of OBA	Optical Bench Assemble	Any loss in MLI thermal-control function due to particle impacts is thought to be negligible, so detection is not possible.	N/A
ISIM	Skirt	Any loss in MLI thermal-control function due to particle impacts is thought to be negligible, so detection is not possible.	N/A
ISIM	ACIS Telescope Shade	Any loss in MLI thermal-control function due to particle impacts is thought to be negligible, so detection is not possible.	N/A
ISIM	Translation Table (+Z/+X side if HRC was in focal position)	The thermal effects of a paint spall when compared to the mission surface degradation is negligible. Were the facesheets penetrated some impact on performance would be expected.	The translation table performance has shown no effect due to the event.
ISIM	ACIS Cold Radiator	The thermal effects of a paint spall when compared to the mission surface degradation is negligible. Were the plate penetrated the radiator performance could be degraded.	ACIS has reported no change in the radiator function.
ISIM	ACIS Sun Shade	Any loss in MLI thermal-control function due to particle impacts is thought to be negligible, so detection is not possible.	N/A
ISIM	-X Surface Turtle Shell	Damage to a single OSR is unlikely to impact the performance of the system, so detection is not possible.	N/A

Search for Previous Events:

With the vehicle state of health verified, the impact region narrowed down, and the possible impact to spacecraft surfaces identified, one question remained. Have we seen an event like this before? To answer that question, a data collection was performed for all times after the most recent Safe Mode event (2000:048) where Chandra was on guide stars for a minimum of four and a half minutes. Defining an event as any time when the RSS of the attitude error components is larger than 5 arcsec, 1391 events were detected. A more detailed data collection was performed for each of the 1391 events. The detailed collection retrieved data for three minutes before and after the event and was designed to identify obvious causes of attitude disturbances. **Table 5** lists the causes considered and the number of events attributed to each cause. Note that the causes can overlap.

Table 5: Nominal Events that Cause Attitude Disturbances

Cause	Explanation	Number Detected
Momentum unloads	Only momentum unload performed in NPM will be detected. For the data collection period 96 unloads were performed in NPM.	96
Translation Table move	SCS 107 moves the Translation Table while in NPM. This will cause an attitude disturbance.	43
Bad Stars	For the automated sorting, a bad stars flag was set if the largest component of the attitude error was in roll AND the mean of the Kalman Score was more than a half. The Kalman score was defined as the number of stars rejected by the Kalman filter at each timestep.	444
HRC Door Moves	When entering or exiting the radiation zone, the HRC door is sometimes moved while in NPM. This is detectable in the pointing stability plots. The MSID for automated detection of HRC door moves is not available in the engineering data, so this field was created by hand and is not an exhaustive list.	14
Special Events	Any event that transitions the spacecraft from standby mode to NMM, re-initializes the Kalman filter or manually fires the thrusters will perturb the pointing stability. These events include: IRU Calibration Uplinks, Bright Star Hold Recovery, Safe Mode Recovery, the IRU swap, the MUPS SOH check and the MUPS calibration. This field was created by hand and is not an exhaustive list.	11
Recent Maneuver	It was noticed that many events were simply settling of errors after a maneuver. The backstop attitude history was used to find the last maneuver end time for each event. Any event within 10 minutes of the end of a maneuver was marked as having a recent maneuver.	250

When all events with one of the above causes were removed, 584 events remained. This is too many events to accurately assess by hand, so a second filtering method was used. The goal was to identify only those events where the attitude error change was impulsive. A gradual change is not indicative of an impact type event.

To accomplish this, a “transient” parameter was defined for every event. This transient was calculated by taking the cumulative sum of the RSS of the attitude error over a 20 second period. The cumulative sum was calculated with a boxcar method. The maximum calculated cumulative sum was declared to be the transient for that event. The cumulative sum causes noise to cancel itself out, and the 20 second period will catch only fast changes in attitude error. Any event with a transient greater than 4 arcsec was marked as a possible impulse type event.

As a sanity check, the events marked as possible impulsive events were compared to the identified causes. Since momentum unloads are impulses, every momentum unload should be marked as a possible impulsive event. Every momentum unload was so marked using this method. Translation moves are also impulsive events; all 43 Translation Table moves were marked using this method.

In total, 475 events were found to have transient values over 4 arcsec. When all of the events with an identified cause were removed 83 remained. These 83 were plotted and checked by hand. **Table 6** shows the results of these checks.

Table 6: Causes Identified through Hand Checks

Cause	Explanation	Number Detected
Bad Stars	The attitude error, the number of Aspect Camera error flags and the number of stars rejected by the Kalman filter were plotted on a single figure. Those instances where a bad star clearly initiated the event were marked as having bad stars.	60
HRC Door Moves	The automated detection of the HRC door move signature did not detect all events. The weekly loads were used to check the remaining events.	5
Special Events	The automated filtering identified disturbances while SCS 107 was running but 12 events were found during the settling time after a SCS 107 trip. The power on of the gyros in IRU-2 also caused a disturbance not anticipated in the initial check of special events.	13
Telemetry Corruption	In one event, the attitude errors instantaneously jumped to very large numbers and then returned to near zero. The magnitude of the error, if seen by the OBC, would have caused a Safe Mode transition.	1
Exceptionally large gravity gradient torque	One event showed a gradual increase in the attitude error and drift in the stars. The event was within thirty minutes of perigee and the system momentum change over the time period was large and consistent with the gravity gradient torque.	1
Unknown, internal, likely stars	One event could not be clearly attributed to stars and showed a change in the amplitude of the spacecraft flexible modes. There was, however, no change in the net system momentum. Therefore, the event is internal. It is likely due to stars, but could be some other internal reconfiguration. No commanding occurred near the time of the event.	1

Cause	Explanation	Number Detected
Impulse	Two impulsive events were found. One on 2003:319 spurred this investigation. The second, on 2002:116 was significantly smaller. It is on the edge of our detection capabilities (0.02 ft-lb-sec change), but there was a change in the net system momentum.	2

Conclusion:

Detailed analysis of spacecraft telemetry shows that Chandra was likely impacted by a micrometeoroid on 15 November 2003. Analysis of subsystem telemetry showed no ill effects on the primary units. A study of the impact area showed that all critical spacecraft units were protected from micrometeoroid impacts or were not in the possible impact region. A search for previous impact type events did return one other such event. This second event was smaller than the event of 2003:319 and is at the limit of our detection capabilities. Like the impact of 2003:319, Chandra appears to have suffered no ill effects due to this second detected potential impact.